AD-A119 107 ROYAL AIRCRAFT ESTABLISHMENT FARNBOROUGH (ENGLAND) F/G 1/3
SOME MEASUREMENTS OF WING BUFFETING ON A FLUTTER MODEL OF A TYP--ETC(U)
JAN 82 D G MABEY, B E CRIPPS
UNCLASSIFIED RAE-TR-82007 DRIC-BR-83884 NL

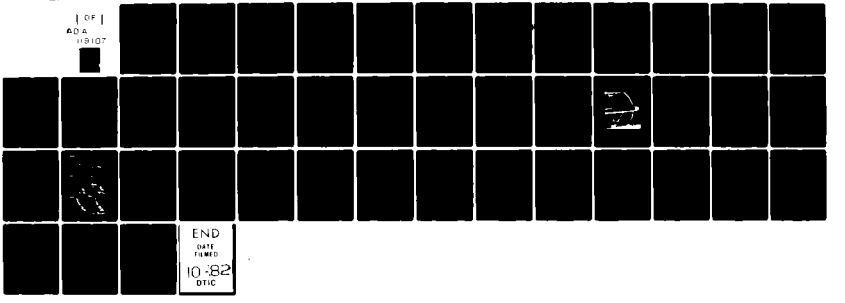

TR 82007

ROYAL AIRCRAFT ESTABLISHMENT

*

Technical Report 82007

January 1982

SOME MEASUREMENTS OF WING BUFFETING ON A FLUTTER MODEL OF A TYPICAL STRIKE AIRCRAFT

by

D. G. Mabey
B. E. Cripps

*

Procurement Executive, Ministry of Defence
Farnborough, Hants

REPORT DOCUMENTATION PAGE

Overall security classification of this page

UNLIMITED

As far as possible this page should contain only unclassified information. If it is necessary to enter classified information, the box above must be marked to indicate the classification, e.g. Restricted, Confidential or Secret.

1. DRIC Reference (to be added by DRIC)	2. Originator's Reference	3. Agency Reference	4. Report Security Classification/Marking
	RAE TR 82007	N/A	UNLIMITED

5. DRIC Code for Originator	6. Originator (Corporate Author) Name and Location
7673000W	Royal Aircraft Establishment, Farnborough, Hants, UK
5a. Sponsoring Agency's Code	6a. Sponsoring Agency (Contract Authority) Name and Location
N/A	N/A

7. Title: Some measurements of wing buffeting on a flutter model of a typical strike aircraft

7a. (For Translations) Title in Foreign Language

7b. (For Conference Papers) Title, Place and Date of Conference

8. Author 1. Surname, Initials	9a. Author 2	9b. Authors 3, 4	10. Date	Pages	Refs.
Mabey, D.G.	Cripps, B.E.		January 1982	41	20

11. Contract Number	12. Period	13. Project	14. Other Reference Nos.
N/A	N/A		Structures BF/B/0893

15. Distribution statement
(a) Controlled by –
(b) Special limitations (if any) –

16. Descriptors (Keywords) (Descriptors marked * are selected from TEST)

Unsteady aerodynamics. Buffeting.

17. Abstract

Some measurements of buffeting were made on a 1/30 scale complete flutter model of the wing of a typical strike aircraft. The tests covered the Mach number range from M = 0.45 to 0.94 and the Reynolds number range from R = 0.6 × 10^6 to 1.7 × 10^6. With a clean wing, buffeting measurements were made over a wide range of Reynolds number at constant Mach number to derive the buffet excitation parameter at the wing fundamental bending frequency of 170 Hz. The complete flutter model had a rigid body freedom of rotation in roll at a frequency of about 39 Hz, and indicated the onset of 'wing rock', well above the buffet onset boundary. The wing rock started close to the maximum limit of buffet penetration achieved in flight. Significant variations in aerodynamic damping were measured with flow separations for both the low frequency roll mode and the higher frequency first wing bending mode. For the roll mode these variations may be predicted by quasi-steady strip theory, but not for the fundamental bending mode. This difference indicates an important frequency effect on the separated flows, particularly at subsonic speeds. These tests indicate some limitations of buffeting measurements on ordinary wind tunnel models, particularly for half models.

F5910/1

RAE Form A143

UDC 533.6.013.43 : 533.693 : 623.746.4

ROYAL AIRCRAFT ESTABLISHMENT

Technical Report 82007

Received for printing 18 January 1982

SOME MEASUREMENTS OF WING BUFFETING ON A FLUTTER MODEL OF A TYPICAL STRIKE AIRCRAFT

by

D. G. Mabey

B. E. Cripps

SUMMARY

Some measurements of buffeting were made on a 1/30 scale complete flutter model of the wing of a typical strike aircraft. The tests covered the Mach number range from M = 0.45 to 0.94 and the Reynolds number range from $R = 0.6 \times 10^6$ to 1.7×10^6. With a clean wing, buffeting measurements were made over a wide range of Reynolds number at constant Mach number to derive the buffet excitation parameter at the wing fundamental bending frequency of 170 Hz. The complete flutter model had a rigid body freedom of rotation in roll at a frequency of about 39 Hz, and indicated the onset of 'wing rock', well above the buffet onset boundary. The wing rock started close to the maximum limit of buffet penetration achieved in flight. Significant variations in aerodynamic damping were measured with flow separations for both the low frequency roll mode and the higher frequency first wing bending mode. For the roll mode these variations may be predicted by quasi-steady strip theory, but not for the fundamental bending mode. This difference indicates an important frequency effect on the separated flows, particularly at subsonic speeds. These tests indicate some limitations of buffeting measurements on ordinary wind tunnel models, particularly for half models.

Departmental Reference: Structures BF/B/0893

LIST OF CONTENTS

		Page
1	INTRODUCTION	3
2	EXPERIMENTAL DETAILS	3
	2.1 Model	3
	2.2 Instrumentation and analysis	4
	2.3 Test conditions	5
3	RESULTS	5
	3.1 Steady bending moment measurements and flow visualisation	5
	3.2 Dynamic strain measurements	7
	3.3 Damping measurements	8
	3.4 Buffet excitation parameter	9
4	DISCUSSION	11
5	CONCLUSIONS	14
Appendix	The calculation of damping from quasi-steady strip theory	15
Tables 1 and 2		17
Notation		18
References		19
Illustrations		Figures 1-21
Report documentation page		inside back cover

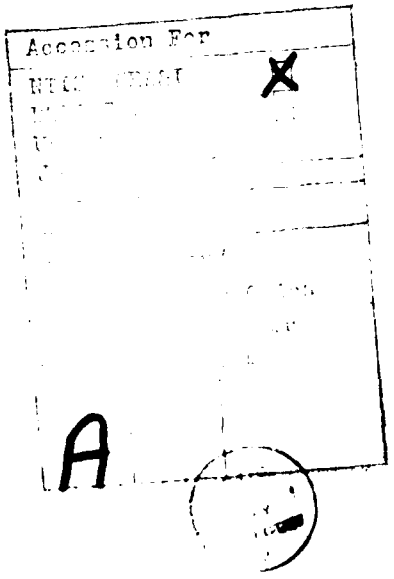

1 INTRODUCTION

The advantages and limitations of using aeroelastic models for buffeting tests were discussed in a previous paper[1]. Two completely different aeroelastic models were selected for a further study of this technique and to provide detailed predictions of buffeting. The tests of the aeroelastic model of a large slender wing transport aircraft, extending into the vortex breakdown region, have already been reported[2]. The tests of the typical strike aircraft are reported here; they confirm the general conclusions of the previous paper[1] that aeroelastic models can provide much more detailed and valuable information about buffeting on aircraft than can ordinary wind tunnel models.

In addition, the present tests show that with the provision of a rigid body freedom of rotation in roll, an aeroelastic model can give a sharp indication of the low frequency 'wing rock' boundary, in addition to wing buffeting. In the United Kingdom the 'wing rock' boundaries are generally derived during measurements of the rigid body dynamic derivatives on ordinary wind tunnel models[3]. In America 'wing rock' boundaries are measured by 'flying' an aeroelastic model on a cable mount system[4], but this is a much more difficult method than that described here.

2 EXPERIMENTAL DETAILS

2.1 Model

Fig 1 shows the flutter model of the wing used for the present experiments installed in the top and bottom slotted working section of the RAE 3ft tunnel. The wing is mounted on a straight cylindrical body, which is totally unrepresentative of the aircraft fuselage. In particular, the body includes no engine nacelles, cockpit canopy or tailplane. The cylindrical body was supported on a 3° cranked sting. This could be rolled to produce either 3° body incidence over a range of sideslip (as in Fig 1), or 3° sideslip over a range of incidence, as well as a range of incidence at zero sideslip, in conjunction with the pitch variation provided by the tunnel quadrant. The wing is set at an angle of 1° to the body axis. Fig 1 shows the wing fitted with scaled slipper tanks, together with a pod on the starboard side. This asymmetric store configuration was of current interest and was selected for the initial series of buffeting measurements at low Reynolds numbers. Most of the test results presented here relate to the clean wing, and cover a wider range of Reynolds number.

A brief description of the wing construction is appropriate, and is quoted from a report by Sowden[5]. "The wing model was structurally based on an idealised interpretation of the full scale aircraft. That is, an outer wing with three box sections welded together, the joints between adjacent boxes corresponding to the wing spars, and an inner wing with one/two box sections. The wing sections were welded to a 'rigid' fuselage spar that was 'rigidly' restrained in all freedoms except roll and this freedom was controlled by a torsion bar arrangement. Construction was of light alloy with a balsa/pine profile and a silk covering. Separate ailerons were fitted with a representative jack stiffness. Ballast weights were embedded during construction to give a representative mass distribution." Fig 1 shows that the surface finish achieved by this method of construction was good, particularly in the leading-edge region, (although the surface finish of the port

wing was superior to the starboard wing). Hence a narrow roughness band was applied to fix transition close to the leading-edge. A slot provided in the cylindrical body allowed the wing to have a maximum roll amplitude of about $\pm 2^{\circ}$ on the torsion bar. For some tests a carefully fitted internal clamp suppressed this freedom in roll.

Although the modal frequencies of the wing mounted in the quadrant of the RAE 3ft tunnel were measured 'wind off' by a frequency sweep technique, the corresponding mode shapes were not measured. However, these mode shapes should not have differed greatly from those measured before the flutter tests[5]. Then the wing was mounted on a long cylindrical pole extending from the maximum section of the tunnel to the diffuser. The symmetric and antisymmetric mode shapes, with the freedom in roll, which are of greatest interest, are reproduced in Fig 2. The frequencies quoted relate to the clean wing and the wing with stores (bracketed figures) in the RAE 3ft tunnel.

2.2 Instrumentation and analysis

The wing response was monitored by six uncompensated strain gauge bridges, three on each wing, provided for the original flutter tests. The static bending moments on both wings were measured by wire strain gauges. In addition the unsteady bending and torsion moments on both wings were measured by semi-conductor strain gauges for greater sensitivity. The separate signals from the port and starboard wings could be added to give the symmetric response and subtracted to give the asymmetric response. This helped to identify the modes excited. This arrangement of separate bridges is contrary to normal practice in buffeting measurements, where pairs of gauges on each wing are wired to give only the symmetric response.

For the unsteady measurements the rms voltage, dV, the bridge energisation voltage, V, and the gauge factor, σ, give the rms strain,

$$\varepsilon = dV/V\sigma \quad . \tag{1}$$

A factor of $\sigma = 120$ was assumed for the semi-conductor gauges. For the static calibration of the wing-root bending moments, known weights were applied at different points on the wings. A rough estimate of the wing normal force coefficient was obtained by assuming that the force acted at the mid-semi span (b/4). The measured bending moments were then reduced to normal force coefficients by dividing by the moment $qSb/8$. For the dynamic calibration, the wing was excited at the fundamental bending frequency with a vibrator, and a linear relationship was established between the rms wing-root strain signal and the rms acceleration, $\ddot{y}$, measured by a light accelerometer attached to the wing tip by double-sided adhesive tape.

The experiment was controlled by monitoring the unsteady signal from the port semi-conductor strain gauge bridge on a Real-Time-Spectrum analyser. For a limited number of conditions the six strain gauge signals were recorded on a tape recorder for subsequent analysis on the Presto computer system[6]. Record lengths of about 120 s were taken, which for the wing first symmetric bending frequency at about 170 Hz gives about 21000 cycles of buffeting. With this large number of cycles of buffeting, and a level of damping

always greater than 1% crictical, good estimates of the total damping can be obtained, using standard methods for analysing random data[7], such as the measurement of half power points.

2.3 Test conditions

The model was tested in the 0.91m wide × 0.64m high top and bottom slotted section of the RAE 3ft tunnel (Fig 1). The Mach number range was from M = 0.45 to 0.94 and the tunnel total pressures, p_t, were 0.34, 0.67 and 0.94 bar. Table 1 lists the test conditions of greatest interest.

The maximum wing incidence of the present tests (Table 1) was intended to be just above the heavy buffeting contour measured during previous buffeting tests on an ordinary wind tunnel model of a similar configuration. This heavy buffeting contour was in good agreement with the maximum flight penetration measured during steady manoeuvres. Generally this maximum incidence could be reached, even for the highest total pressure selected, without exceeding the estimated safe normal force limit of 700 N (157 lb) on each wing of the model. However, with the freedom in roll the maximum incidence (14^o) could not be achieved at M = 0.60 at the highest total pressure, because of the alarming amplitude of the 'wing rock'. When previously tested at zero incidence at transonic speeds, this model had been flutter-free at a total pressure of 3.5 bar. The reduced stiffness of the model was such that this test demonstrated the 30% flutter margin required for the aircraft at sea level conditions.

A roughness band was applied to fix transition at a streamwise distance x_k = 5 mm from the leading-edge of the wing. The roughness band was 2.5 mm wide and was formed by a sparse distribution of ballotini (small glass spheres) with a diameter, k = 0.1 mm. This diameter was selected[8] to fix transition at the intermediate total pressure p_t = 0.67 bar, and hence to somewhat 'over-fix' transition at p_t = 0.94 bar. Most of the scale effect observed between p_t = 0.67 bar and 0.34 bar was probably due to the 'under-fixing' of the boundary layer at the lower total pressure.

3 RESULTS

3.1 Steady bending moment measurements and flow visualisation

For the clean wing the steady bending moment coefficients measured without and with the roll freedom (Figs 3 and 4 respectively) are generally almost the same over a wide range of total pressures. This indicates that the deflection between the wing and the cylindrical body is generally unchanged when the clamp is removed, permitting the roll freedom. However, closer inspection shows that the variation of the steady bending moment coefficient with total pressure is more noticeable without the roll freedom (Fig 3) than with the roll freedom (Fig 4).

Thus Fig 3 shows that at M = 0.60 both the initial slope, and the level at the stall, are lower at the lowest total pressure than at the two higher pressures. In contrast, at M = 0.80 the initial slope is identical although the levels at the stall are different. These differences are unlikely to be caused by static aeroelastic distortion, because this would be expected to alter the initial slopes both at M = 0.80 and 0.86, as

well as at M = 0.60. Hence the differences observed at M = 0.60 and 0.80 must be attributed to genuine adverse scale effects, particularly at the lowest Reynolds number (only about 0.5×10^6), when transition is 'underfixed', as discussed above in section 2.3.

Figs 3 and 4 show a significant increase in the slope from M = 0.60 to 0.80, and a further small increase at M = 0.86. These variations in the bending moment coefficient, measured with a large cylindrical fuselage, are appreciably smaller than the corresponding variations in lift curve slope measured on another model with a representative fuselage, and thus may indicate an 'interference' effect common to all the measurements, or an inboard movement of the centre of lift sensed by the moment gauges, or a combination of these effects.

Figs 3 and 4 also include the angle of incidence for buffet onset at every Mach number, derived from the unsteady component of the wing-root bending moment. These angles of incidence do not vary significantly with total pressure, so that scale effects on buffet onset are small. The incidences for buffet onset are well within the linear range of the steady bending moment measurements. This result confirms previous findings[9] that sudden changes in lift curve slope often indicate the sudden growth of small separations (and therefore heavy buffeting), rather than the onset of separations (and light buffeting).

When the wing was fitted with the store configuration, measurements were made only at the lowest total pressure (0.34 bar). This restriction was applied because of the risk of damaging the stores under steady asymmetric loads or buffeting conditions. The main effect of the stores on the steady bending moments was to increase the zero lift angle by about 0.6°, although there were changes in the development of the stall, particularly at M = 0.60 (Fig 5). These differences were not investigated, because of the low Reynolds number of the tests.

The development of the separation at and after buffet onset was shown by oil flow photographs taken at the highest total pressure. The separations on the port wing were a little smaller than those on the starboard wing (because of the superior finish on the port wing) and are shown in Fig 6.

For a Mach number of 0.60, buffet onset occurs at $\alpha = 9^\circ$. The flow separates close to the leading-edge at about 80% semi-span, forms a tiny bubble and then immediately reattaches. The flow is attached both inboard and outboard of this bubble. An increase in incidence to $\alpha = 11^\circ$ produces a rapid extension of this bubble, downstream towards the trailing-edge and spanwise towards the wing-tip and the wing root. It is interesting to note that the bubble still does not extend to the trailing-edge, and that there are four discrete cells visible under the main shear layer. The span of every cell is roughly equal to its length. Well ordered structures of this kind are often observed at subsonic speeds even under nominally two-dimensional bubbles. Lateral movement at low frequencies of these cells could well excite the 'wing-rock' phenomenon to be discussed in section 4. This phenomenon is much more serious at M = 0.60, when there is a well defined cellular structure under the separation, than at higher Mach numbers, when such a structure is not observed.

For a Mach number of 0.80, buffet onset occurs at $\alpha = 4^{o}$. The flow separates at a shock on the outboard wing (located at about x/c = 0.25, from about 60 to 90% of semi-span) and immediately reattaches. An increase in incidence to $\alpha = 7^{o}$ moves the shock forward towards the leading-edge, while the separation extends downstream towards the trailing-edge. The direction of the complex separated flow behind the shock is predominantly spanwise. Close inspection of the flow on the inboard section of the wing reveals a weak, oblique shock starting from the apex. This oblique shock is a classic feature of the transonic flow on a swept wing of finite aspect ratio, and was discussed by Rogers et al[10].

For a Mach number of 0.86 the separation development is similar to that described at M = 0.80, but occurs more rapidly. Buffet onset is at $\alpha = 3^{o}$, and by $\alpha = 5^{o}$ the shock induced separation is as extensive as at $\alpha = 7^{o}$ at M = 0.80. The oblique shock starting from the apex in the wing is stronger than at M = 0.80 and hence is more noticeable.

3.2 Dynamic strain measurements

The symmetric or antisymmetric modes excited can be found by respectively adding or subtracting the port and starboard wing-root strain signals, as discussed in section 2.2. The time histories of these combined responses may then be analysed by the Presto computer system[6], and conveniently displayed as spectra with linear scales (Fig 7).

For a typical heavy buffeting condition (M = 0.60, $\alpha = 14^{o}$), the response in the symmetric modes is virtually the same with or without the roll freedom, and consists of first symmetric bending at 174 Hz (Fig 7a). This result is reasonable because the boundary condition for the symmetric modes is unaltered by the roll constraint. Hence the symmetric component in the excitation spectrum must excite the same response. However, for the corresponding response in the antisymmetric modes, there are inevitably large differences, because here the boundary conditions are radically different, even if the antisymmetric excitation spectrum is unaltered by the motion (as is most likely). Without the roll freedom the only antisymmetric mode excited significantly is the first antisymmetric bending at 155 Hz, which must involve some twisting of the sting. In marked contrast, with the roll freedom the rigid body roll at 40 Hz is excited, together with a combined antisymmetric bending and torsion mode at 251 Hz (Fig 7b). (These modes probably involve little twisting of the sting.) For these antisymmetric modes the results for the wing with the roll freedom give a better approximation to the aircraft, which does have something like a freedom in roll. On the aircraft the Dutch Roll frequency is about 0.5 Hz, which would correspond with about 15 Hz for this 1/30 scale model. Hence the frequency parameter for the roll mode in the present tests is too high.

Two further observations can be made from Fig 7. Firstly, there is significant forced model response (both symmetrically, and antisymmetrically) at low frequencies (say less than 10 Hz), where there are certainly no structural modes. This observation indicates that a comparatively high level of excitation at low frequencies is provided by the flow separations on the model. (The level of response is about five times higher than that excited by the flow unsteadiness in the wind tunnel at zero incidence.) Secondly, because of strain gauge misalignment and differences in sensitivity, the

spectrum of the symmetric modes includes a faint indication of the antisymmetric mode at 251 Hz (Fig 7a), and the spectrum of the antisymmetric modes includes a clear indication of the first symmetric bending mode at 174 Hz (Fig 7b). Subsequent analysis of the buffeting measurements is concentrated on the large response in the first symmetric bending mode, followed by brief comments on the two antisymmetric modes.

Fig 8 shows the variation of rms unsteady wing-root strain, ε , in the first bending mode, as a function of the angle of incidence for three Mach numbers and total pressures. Buffet onset is sharply defined at M = 0.60 (with the leading-edge separation) and at M = 0.86 (with the strong shock induced separation). However at M = 0.80 buffet onset is less well defined and caused by the slow initial extension downstream of the separation behind the shock wave. Buffet onset curves of this type, with a sudden initial rise in response, followed by a constant level before a further increase, are frequently observed on swept wings close to the boundary along which the flow changes from a leading-edge to a shock induced separation.

Early investigations[11] of the similarity laws for buffeting suggested that in the absence of scale effects:

$$\varepsilon \propto \rho^{\frac{1}{2}} \quad - \text{ for aerodynamic damping ,} \tag{2}$$

or

$$\varepsilon \propto \rho \quad - \text{ for structural damping .} \tag{3}$$

There must be appreciable scale effects because neither of these power laws is appropriate to these measurements. In addition we shall see later (section 3.3) that the total damping is a combination of aerodynamic and structural damping.

The strain measurements with the roll freedom are believed to correspond most closely with an aircraft in flight. Hence the damping and buffet excitation parameters subsequently presented refer to this condition.

3.3 Damping measurements

From the long signal records, well defined spectra of the buffeting measurements could be obtained (*eg* Fig 7), as discussed above in section 2.2. From these spectra total damping estimates (per cent critical) could be readily obtained, using the half power point method. The buffeting spectra for the symmetric modes indicate two interesting trends in the damping measurements for the first bending mode at about 174 Hz (Fig 9).

(a) For constant Mach number and angle of incidence the damping increases with the total pressure (*ie* the stream density), in accordance with theory.

(b) For constant Mach number and total pressure damping increases with the angle of incidence, the increase being most marked after the onset of buffeting. This trend is most obvious at M = 0.60: its significance will be discussed in section 4. Fig 10 shows the total damping measurements at two angles of incidence: ($\alpha = 1^{\circ}$ and the incidence for maximum buffet penetration) plotted against the product of the freestream density and the freestream velocity. In addition to the trends shown by Fig 9, Fig 10 shows that the wind-on damping measurements are consistent with a

constant structural damping coefficient of g/2 = 0.8% critical, as measured wind-off in a ground resonance test.

The total damping for the symmetric overtone bending mode at about 550 Hz is predominantly structural, (g/2 = 2% critical) and only varies a little with freestream density and velocity. The variation with angle of incidence is within the scatter of the measurements (Fig 11). Similar remarks apply for the first anti-symmetric structural mode at about 250 Hz (Fig 12): this mode represents combined bending and torsion.

The roll motion was not significantly excited by the tunnel unsteadiness. Hence for attached flow conditions below the buffet boundary, no damping values could be derived from the antisymmetric wing-root strain records. However roll motion was excited after buffet onset, and a few total damping measurements, typically about 15% critical, were obtained at high angles of incidence (Fig 13). The measurements at the higher tunnel pressures at M = 0.60 and 0.80 are most reliable, because here the model response was largest. These measurements suggest that the total damping in this mode falls as angle of incidence increases. This trend is consistent with that generally observed in derivative measurements and with estimates presented in section 4: the variation is directly due to the flow separation on the outboard wing section. No clear variation of total damping with stream density can be established, although the measurements at the highest density are consistent with a structural damping coefficient, g/2 about 4% of critical, as measured in a previous ground resonance test.

Brief comparative tests at zero sideslip at $p_t = 0.34$ (not presented) indicated that the addition of the antisymmetric wing store configuration had no significant effect on the damping measurements in either the symmetric or antisymmetric modes.

3.4 Buffet excitation parameter

From the strain and damping measurements presented above, the buffet excitation parameter, $\sqrt{nG(n)}$, can now be calculated[12] for the modes of interest according to the relation:

$$\sqrt{nG(n)} = \left(\frac{2}{\sqrt{\pi}}\right)\left[\frac{m\ddot{y}}{qS}\right]\zeta^{\frac{1}{2}} \qquad (4)$$

where m = generalised mass in mode,
$\ddot{y}$ = rms wing tip acceleration in mode,
q = freestream kinetic pressure,
S = wing area,
and ζ = total damping in mode (fraction of critical).

A simple linear relation between the rms wing-tip acceleration measured with an accelerometer and the wing-root strain signal was obtained during a ground resonance test.

Fig 14 shows the buffet excitation parameter derived for the first bending mode for the principal test conditions. Buffet onset is sharply defined, as in the unsteady strain measurements (Fig 8). For a given Mach number the buffet excitation parameter is identical for the two highest pressures, confirming that scale effects are small when

the boundary layer transition is correctly fixed. However the buffet excitation parameter is appreciably higher at the lowest total pressure, presumably because the flow separations are larger when transition is not correctly fixed.

The level of the buffet excitation parameter (about 1.0×10^{-3} to 1.5×10^{-3}) at low angles of incidence, $\sqrt{nG_0(n)}$, before the onset of separations on the wing is a measure of the combined excitation provided by the local flow round the model and the flow unsteadiness in the wind tunnel. Since the flow unsteadiness on an ordinary wind tunnel model at transonic speeds normally produces a lower buffet excitation parameter (only about 0.5×10^{-3} to 0.7×10^{-3}), the additional excitation must be attributed to the pressure fluctuations generated by the separation on the unfaired base of the large fuselage. Thus for this model it would have been impossible to use the flow unsteadiness in the tunnel as a measure of the excitation due to buffeting[9], even at subsonic speeds. The buffet excitation parameter appropriate to the wing flow separations alone may be obtained by subtracting the contribution at low angles of incidence. It is reasonable to assume that shortly after buffet onset there is no correlation between the flow separations on the wing and the excitation at low lift, so that the buffet excitation parameter for the wing separations alone, $\sqrt{nG_1(n)}$, is given by:

$$\sqrt{nG_1(n)} = \sqrt{nG(n) - nG_0(n)} \quad . \tag{5}$$

Equation (5) and Fig 14 show that the maximum level of $\sqrt{nG_1(n)}$ achieved during the present tests is about 3×10^{-3} at M = 0.60 and 0.80, falling to about 2×10^{-3} at M = 0.86. These levels are typical of those achieved on ordinary wind tunnel models (Fig 16), and on aircraft in flight[13,14].

In contrast to the present model, the aircraft has a streamlined rear fuselage, so that in flight the buffet excitation parameter at low angles of incidence is determined by atmospheric turbulence and the aerodynamic and mechanical excitation provided by the engines. Previous tests[13,14] suggest that the sum of these contributions is normally quite small (typically about 0.1×10^{-3} to 0.2×10^{-3}), so that correction according to equation (5) should not be necessary for flight buffeting measurements.

The buffet excitation parameter was also derived for the rigid body roll motion at high angles of incidence, for the few conditions where measurements for the total damping in roll were available. For this mode the measurements are not sufficiently numerous to establish systematic trends for the variation of buffet excitation parameter with angle of incidence, Mach number or total pressure. However the measurements indicate that the buffet excitation parameter in this very low frequency, antisymmetric rigid body mode is of the same order as that for the wing first symmetric bending mode. Further discussion of these results is deferred to section 4.

Equation (4) also provides a good correlation of the small responses in both the combined antisymmetric torsion/bending mode and the symmetric overtone bending modes (at about 250 and 550 Hz respectively). Fig 15 shows some typical results (for M = 0.60) plotted to an arbitrary scale. There are no features of sufficient interest to justify

the additional labour of calibrating the wing-root strain gauges and measuring the generalised masses in these modes, to establish the absolute levels of the buffet excitation parameter.

4 DISCUSSION

For the prediction from wind tunnel tests of the buffet characteristics of new combat aircraft it is important to establish how the levels of buffet excitation parameter measured in wind tunnels compare with flight measurements. In addition it must be possible to scale measured damping coefficients from tunnel to flight and to be certain that all structural modes are correctly represented.

For the present flutter model and the first symmetric bending mode the maximum penetration in the tunnel corresponds with a level of $\sqrt{nG_1(n)} = 3 \times 10^{-3}$ at M = 0.60, falling to about 2×10^{-3} at M = 0.86 (Fig 14). However for the tunnel tests the maximum incidence (Fig 16a) was restricted by the normal force on the model, whereas in flight somewhat higher angles of incidence were achieved, particularly in transient pull ups at the higher Mach numbers (Fig 16b). Hence it is reasonable to infer that if the normal force restriction had been overcome, levels of $\sqrt{nG_1(n)} = 3 \times 10^{-3}$ would have been achieved on the model over the full Mach number range from M = 0.60 to 0.86. No comparative measurements of the buffet excitation parameter are available from the flight tests of this aircraft.

For ordinary wind tunnel models the maximum level of the buffet excitation parameter in the first symmetric bending mode is again about 3×10^{-3}, and this level is comparable with that achieved in flight at much the same angles of incidence. Fig 17 illustrates this by the only measurements available which relate to a TACT F1-11 (for two different angles of wing sweep), a small fighter aircraft and a 65° delta wing. Hence it is reasonable to propose new criteria for the buffet excitation parameter, to supplement those derived previously from buffeting coefficients[14] (Table 2).

As previously remarked[15], the correlations established between dimensionless buffet excitation parameters or buffeting coefficients and the maximum flight penetration are at first sight surprising, because it might reasonably be expected that the severity of buffeting in flight would be based on the dimensional level of vibration (either estimated by the pilot or measured with an accelerometer). However in general the severity of wing buffeting is rarely a controlling factor. The pilots of fighter or strike aircraft often fly right up to a handling boundary, such as pitch/up or stalling, irrespective of the level of buffeting. For the present tests the alarming amplitude of the 'wing-rock' at an angle of incidence of 14° at M = 0.60 and the highest total pressure, suggest that the handling boundary for this wing is determined primarily by a sudden fall in the derivative ℓ_p, the damping due to roll, or even to its reversal in sign. This explanation is consistent with estimated damping measurements, which are presented later (Fig 19).

Low frequency rigid body derivatives are normally measured by the forced oscillation technique[3], for both attached and separated flows. Hence the buffet excitation parameter in these modes due to the separated flows is never measured. During the

present tests the buffet excitation parameter for the roll mode was measured for the first time, and found to be of the same order of magnitude as that for the first symmetric bending mode. However the roll mode is not excited until the moderate buffeting criterion for the first symmetric bending is exceeded (Fig 18). This observation implies that somewhat larger separations, with a higher level of excitation at low frequencies, are required for the roll mode to be excited significantly. Fig 18 also suggests that the buffet excitation parameter at this low frequency remains bounded even at high angles of incidence. Hence according to equation (4), the large roll responses observed briefly at high angles of incidence probably correspond with small or negative values of damping, as suggested above.

The aerodynamic damping for the low frequency rigid body roll mode at 40 Hz may be estimated by quasi-steady strip theory, as described in the Appendix. With attached flow and for small angles of incidence these estimates are in excellent agreement with estimates from the constant value $\zeta_p = -0.40$, obtained from data sheets (Fig 19). For large angles of incidence the strip theory predicts a sudden loss of damping about 3° to 4° above buffet onset, due to the large changes in the spanwise load distribution caused by flow separation. The incidence at which this loss of damping occurs is roughly intermediate between that for the maximum flight penetration in steady turns and transient pull-ups (Fig 16b). This incidence corresponds also with the heavy buffeting limit for the first symmetric bending mode derived from previous tunnel tests on an ordinary wind tunnel model (Fig 16a). (This observation supports the previous remarks about the correspondence between traditional buffeting criteria and aircraft handling boundaries.)

On a wind tunnel model the aerodynamic damping cannot be measured independently of the structural damping. For this aeroelastic model the structural damping, g/2, in the roll mode is believed to be as high as 4% critical, as in the previous flutter tests. If this value is assumed constant and subtracted from the total damping measurements (Fig 13), to give the 'measured' aerodynamic damping, these values are in fair agreement with the estimates from quasi-steady strip theory (Fig 19). In particular, the measurements at M = 0.60 and 0.80 confirm a loss of damping as the angle of incidence and the area of separated flow on the wing increase.

For M = 0.60 and 0.80, Fig 19 also includes a few estimates of damping in the roll mode inferred from 1G flight at different altitudes. These are in excellent agreement with both estimates at M = 0.60, but naturally can provide no indication of the loss of damping at the handling limits.

The aerodynamic damping for the higher frequency, first symmetric bending mode at 174 Hz may also be estimated by quasi-steady strip theory (Appendix) and compared to the measurements. (The aerodynamic damping measurements are derived from the total damping measurements given in Fig 9, subject to the reasonable assumption derived from Fig 10 that the structural damping coefficient, g/2, is 0.8% critical and constant.) With attached flow for small angles of incidence the estimates are in good agreement with the measurements. However, after buffet onset the estimates suggest a fairly rapid fall in aerodynamic damping (Fig 20), just as the estimates for the aerodynamic damping in the

roll mode (Fig 19). In marked contrast the measurements show a significant increase in aerodynamic damping, particularly at M = 0.60. The good agreement between the estimates and the measurements below buffet onset suggests that frequency effects on the thin attached boundary layers are small. The large discrepancy between the theory and the measurements after buffet onset suggests that frequency effects on the thick separated shear layers are large, so that the use of quasi-steady theory is no longer justified. Fig 20 suggests that these frequency effects are much larger at M = 0.60 with a large area of separated flow (from the leading-edge) than at M = 0.80 and 0.86 with a smaller area of separated flow (from the shock).

In addition to the global effect of the smaller areas of separated flow at transonic speeds, another factor probably limits the variation of aerodynamic damping with angle of incidence for aircraft structural modes. The aerodynamic damping at transonic speeds is naturally strongly influenced by the movement of shock waves. Now for inviscid transonic flows Nixon has shown[16] that although large changes of shock wave motion and phase angle occur at the very low frequency parameters appropriate to rigid body modes, frequency effects stabilise for frequency parameters appropriate to structural modes, as low as $\omega\bar{c}/U = 0.3$, or $f\bar{c}/U = 0.05$. Hence within the inviscid transonic flowfield upstream of the shock there is a powerful control applied to limit the high frequency effects produced within the area of separated flow downstream of the shock. Further evidence for the existence of this powerful control is provided by recent measurements[17] on a NACA 64A010 aerofoil pitching about its quarter chord point at a Mach number of 0.80 and a Reynolds number of 12×10^6. Comparison of the unsteady pressure measurements at $\alpha = 0^\circ$ (when the flow is attached) and at $\alpha = 4^\circ$ (when the flow is separated) show that for frequency parameters lower than about $\omega c/U = 0.5$ incidence effects due to flow separations are large, whereas above $\omega c/U = 0.5$ incidence effects are small (Ref 17, eg Figs 17 and 22). These comparisons are relevant to the present measurements shown in Figs 19b and 20b although the thickness/chord ratio of the wing is lower than for the aerofoil, varying from 8% at the kink to 6% at the tip.

For the higher frequencies of the symmetric overtone bending and the combined antisymmetric bending/torsion modes the damping variations with angle of incidence are negligible both at M = 0.80 and 0.86 (Figs 11 and 12), consistent with the suggestions made above. In addition at these higher frequencies there is no significant influence of flow separations on the damping at subsonic speeds. This is a feature of the results which deserves investigation in a future experiment.

Aerodynamic damping measurements on a model may be extrapolated to an aircraft according to the equation given by Jones[12], if scale effects on the separations are neglected. Scale effects are generally small for the large separations associated with heavy buffeting although they are often large close to the buffet boundary. An advantage of making buffeting measurements on aeroelastic models is that they usually produce significant aerodynamic damping (eg about 3% critical for $p_t = 0.94$ bar in Fig 10). The damping ratio, ζ_a/ζ_m, required to extrapolate from an aeroelastic model to full scale is typically only about 3. In contrast, on an ordinary wind tunnel model the aerodynamic damping ratio is often as low as 1% critical (not measured accurately because of

the difficulty of estimating the wind-on structural damping). The damping ratio, γ_a/γ_m is typically as high as 9. Hence the full scale aerodynamic damping ratio (typically about 9% critical) can be estimated more accurately from tests on aeroelastic models than on ordinary wind tunnel models.

Finally we must re-emphasise[1] that a half model can only simulate symmetric response modes of a real aircraft. A complete model must be used if antisymmetric modes are to be simulated. For buffeting measurements on a complete model it is advantageous to measure the port and starboard wing-root strain signals independently. These signals may then be added or subtracted electronically to obtain the symmetric or antisymmetric responses, as illustrated in Fig 7. For an ordinary sting supported complete model this technique should produce fair estimates of the buffet excitation parameter both for the rigid body roll mode and the first symmetric bending mode, even if the frequency parameters are not correct. However for higher frequency structural modes some differences are inevitable because of large differences in frequency parameter and mode shape.

Despite these caveats Butler has predicted[18] the symmetric torsional response in flight on a TACT F1-11 aircraft from tests on a half model at a frequency parameter $f\bar{c}/U = 0.35$. The maximum level of the buffet excitation parameter for this mode was about $\sqrt{nG_1(n)} = 0.0055$, comparable with that for the first symmetric bending frequency $\sqrt{nG_1(n)} = 0.0025$.

5 CONCLUSIONS

Buffeting measurements on a flutter model of the wing of a typical strike aircraft suggest five main conclusions.

(1) Sufficient measurements of the buffet excitation parameter for the first symmetric bending mode have now been obtained to formulate new criteria for the severity of buffeting in flight. These new criteria supplement previously determined buffeting coefficients (Table 2).

(2) The buffeting coefficients previously determined from wind tunnel tests derive from aircraft handling boundaries, rather than from any quantitative assessment of buffeting by the pilot.

(3) On this wing the handling boundary at high angles of incidence is probably 'wing rocking' caused by a sudden loss in the damping due to roll (Fig 19). The buffet excitation parameter in this mode remains bounded at high angles of incidence and comparable with that in the first symmetric wing bending (Fig 18).

(4) Significant variations on aerodynamic damping occur after the onset of flow separations. For the low frequency rigid body roll mode these variations may be explained by the spanwise changes in loading predicted by quasi-steady strip theory (Fig 19). For the higher frequency first symmetric bending mode, this method is not adequate, owing to a strong frequency effect on the separated flow (Fig 20).

(5) Although half models can predict the symmetric buffeting response of aircraft, complete models are needed to predict both symmetric and antisymmetric responses (Fig 7).

Appendix

THE CALCULATION OF DAMPING FROM QUASI-STEADY STRIP THEORY

The measurements of aerodynamic damping in the first symmetric bending mode on this flutter model show a significant increase after the onset of flow separations (Fig 9). Similar, although smaller variations have been observed also on ordinary wind tunnel models[9,13,14]. These variations in aerodynamic damping have not yet been explained convincingly.

Lambourne suggested[19] that such variations might be explained by spanwise variations in the local quasi-steady normal force curve slopes, $(dC_N/d\alpha)_\eta$, following flow separations. He calculated that on a typical swept-wing (a Warren 12 planform) the change in the spanwise loading caused by flow separation would first produce a large increase (100%) in aerodynamic damping, followed by a sudden fall in damping as the angle of incidence increased. In a subsequent experiment on an ordinary wind tunnel model of a Warren 12 wing no significant variation in aerodynamic damping was detected. However this experiment was inconclusive because the maximum predicted aerodynamic damping was small relative to the structural damping (about 1% critical as usual). The present experiments provide a better test for the hypothesis because both the measured and predicted variations in aerodynamic damping are much larger.

Following Lambourne's notation[19], the aerodynamic damping may be written as:

$$\gamma(\%\ \text{critical}) = \left[\frac{1}{4}\frac{\rho s \bar{c}^2}{m}\left(\frac{V}{\omega \bar{c}}\right)\right] I \ , \qquad \text{(A-1)}$$

where

$$I = \int_0^1 \left(\frac{dC_N}{d\alpha}\right)_\eta \left(\frac{c_\eta}{\bar{c}}\right) f^2(\eta)\, d\eta \ , \qquad \text{(A-2)}$$

and

$$f(\eta) = \text{mode shape of interest} \ . \qquad \text{(A-3)}$$

The ground resonance test of the flutter model suggested that the first symmetric bending mode could be approximated by:

$$f(\eta) = \eta^2 \ . \qquad \text{(A-4)}$$

For this wing, spanwise normal force distributions were obtained for η = 0.32, 0.55, 0.69, 0.82 and 0.95 from unpublished static pressure measurements[20] on a large half model tested in the ARA 9ft × 8ft tunnel at a Reynolds number of 4.5×10^6.

The results of typical calculations are shown in Fig 21. The product of the normal force coefficient and the local chord ratio at η = 0.82 indicates the first sudden change in loading (indicative of transonic flow) for an angle of incidence of about 4°. For higher angles of incidence the changes in loading extend inboard and outboard from this position (Fig 21a). The ordinate for the integral, I , (equation (A-2)) can be derived from these curves (Fig 21b). Equation (A-4) ensures that the aerodynamic damping is dominated by the wing sections closest to the tip because it contains terms in η^4

in the integrand. The integral increases a little close to buffet onset, and then falls suddenly (Fig 21c). This type of variation is roughly comparable with that predicted by Lambourne for the Warren 12 wing.

The data shown in Fig 21a may be used also to calculate the aerodynamic damping in the rigid body roll mode. For this mode:

$$f(\eta) = \eta \ . \qquad \text{(A-5)}$$

The aerodynamic damping in this mode is not quite so sensitive to wing sections close to the tip, because the integrand now contains terms in η^2 , instead of η^4 . However, the shape of the integral still generally resembles Fig 21c. (This may be seen by comparing Figs 19c and 20c.)

We have already discussed the detailed results of these calculations (section 4). For the low frequency roll mode the method gives fair predictions for the attached and separated flow regions. However, for the high frequency first symmetric bending mode the method gives good predictions for the attached flow, but completely the opposite trend to the measurements for the separated flow. This radical difference in character shows that for separated flows the quasi-steady theory can only be used to explain measured damping variations for very low, rigid body frequencies.

Table 1

TEST CONDITIONS

Mach number M	Total pressure p_t		Reynolds number	Kinetic pressure	Frequency parameter	Maximum wing incidence
	kN/m^2	bar	$R(\times 10^{-6})$	$q(kN/m^2)$	$f\bar{c}/U$ (170 hz)	(^{o})
0.60	33.7 67.4 94.3	0.34 0.67 0.94	0.5 1.0 1.4	6.7 13.3 18.6	0.107	14
0.80	33.7 67.4 94.3	0.34 0.67 0.94	0.6 1.2 1.7	9.2 19.8 27.7	0.083	9
0.86	33.7 67.4 94.3	0.34 0.67 0.94	0.6 1.2 1.7	10.8 21.6 30.2	0.078	7

$S = 5.22 \times 10^{-2}\ m^2$

$b = 430$ mm, $\bar{c} = 122$ mm

Roughness $k = 0.1$ mm dia ballotini

$x_k = 5$ mm

Table 2

BUFFET PENETRATION CRITERIA FOR FIRST SYMMETRIC WING BENDING

Severity of buffeting	Buffet excitation parameter $\sqrt{nG_1(\cdot)}$	Buffeting coefficient C''_B (Ref 15)
Light	0.00075	0.004
Moderate	0.00150	0.008
Heavy	0.00300	0.0160

NOTATION

B_1, B_2	port and starboard wing-root strain signals
b	wing span (430 mm)
c	local chord
$\bar{c}$	average chord (122 mm)
C_B	steady bending moment coefficient
C''_B	buffeting coefficient (defined in Ref 14)
f	frequency (Hz)
g/2	structural damping coefficient (% criteria)
k	roughness height
ℓ_p	rolling moment due to rate of roll
M	Mach number
m	generalised mass in mode
$n = f\bar{c}/U$	frequency parameter
$\sqrt{nG(n)}$	buffet excitation parameter due to wing flow separations and flow unsteadiness at zero lift
$\sqrt{nG_0(n)}$	buffet excitation parameter due to flow unsteadiness at zero lift
$\sqrt{nG_1(n)}$	buffet excitation parameter due to wing flow separations
q	kinetic pressure
R	Reynolds number based on $\bar{c}$
S	wing area
s	semi-span
U	free stream velocity
dV, V	rms and steady voltages
x	streamwise distance from leading-edge
α	wing incidence (^{o})
γ	aerodynamic damping (% critical)
ε	rms wing-root strain
σ	gauge factor
ρ	free stream density

Subscript

m	model
a	aircraft

REFERENCES

No.	Author	Title, etc
1	D.G. Mabey	Some remarks on the use of aeroelastic models in buffeting tests. RAE Technical Memorandum Structures 880 (1978)
2	D.G. Mabey C.W. Skingle	Some measurements of buffeting on an aeroelastic model of a slender wing aircraft. RAE Technical Memorandum Structures 942 (1978)
3	C.O. O'Leary	Wind tunnel measurements of aerodynamic derivatives using flexible sting rigs. AGARD LS 114 "Dynamic Stability Parameters", March 1981
4	W.H. Reed F.T. Abbot	A new 'free-flight' mount system for high-speed wind-tunnel flutter models. Proc of Symposium on Aeroelastic and Dynamic Modelling Technology, RTD-TDR-63-4197 Part I, USAF, pp 169-206, March 1964
5	R.A. Sowden	Utilisation of wind-tunnel turbulence for model excitation. BAe unpublished, 1980
6	B.L. Welsh D.M. McOwat	Presto: a system for the measurement and analysis of time-dependent signals. RAE Technical Report 79135 (1980)
7	J.S. Bendat A.G. Piersol	Random data: analysis and measurement procedures. Wiley, New York (1971)
8	A.L. Braslow E.C. Knox	Simplified method for determination of critical height of distributed roughness particles for boundary layer transition at Mach numbers from 0 to 5. NACA TN 4363, September 1958
9	D.G. Mabey	Beyond the buffet boundary. J. Roy. Aero. Soc., April 1973
10	I.M. Hall E.W.E. Rogers	The flow pattern on a tapered swept-back wing at Mach numbers between 0.6 and 1.6. ARC 19691, R&M 3271 (1957)
11	W.B. Huston A.G. Rainey A. Gerald T.F. Baker	A study of the correlation between flight and wind-tunnel buffet loads. NACA RML 55E 16b, 1955
12	J.G. Jones	A survey of the dynamic analysis of buffeting and related phenomena. RAE Technical Report 72197 (1973)
13	G.F. Butler G.R. Spavins	Preliminary evaluation of a technique for predicting buffet loads in flight from wind-tunnel measurements on models of conventional construction. RAE Technical Report Aero 1698 (1976)

REFERENCES (concluded)

No.	Author	Title, etc
14	G.F. Butler G.R. Spavins	Wind-tunnel/flight comparison of the levels of buffeting response intensity for the TACT F-111. Symposium on Transonic Aircraft Technology, AFFDL TR 78-100, August 1978
15	D.G. Mabey	An hypothesis for the prediction of flight penetration of wing buffeting from dynamic tests on wind-tunnel models. ARC CP 1171, (1971)
16	D. Nixon	On unsteady transonic shock motions. AIAA J. Vol 17, No.10, p 1143-1145
17	S.S. Davis G.N. Malcolm	Experiments in unsteady transonic flow. AIAA Paper 79-0769, April 1979
18	G.F. Butler G.R. Spavins	Wind-tunnel/flight comparison of the buffeting response of the TACT F-1-11 transonic research aircraft. RAE Technical Report (in preparation)
19	N.C. Lambourne	Some remarks on the aerodynamic damping appropriate to wing buffeting. RAE Technical Memorandum Structures 871 (1975)
20	T.E. Bateman	Unpublished ARA wind-tunnel tests (1958)

Fig 1 Flutter model in RAE 3 ft tunnel

Fig 2

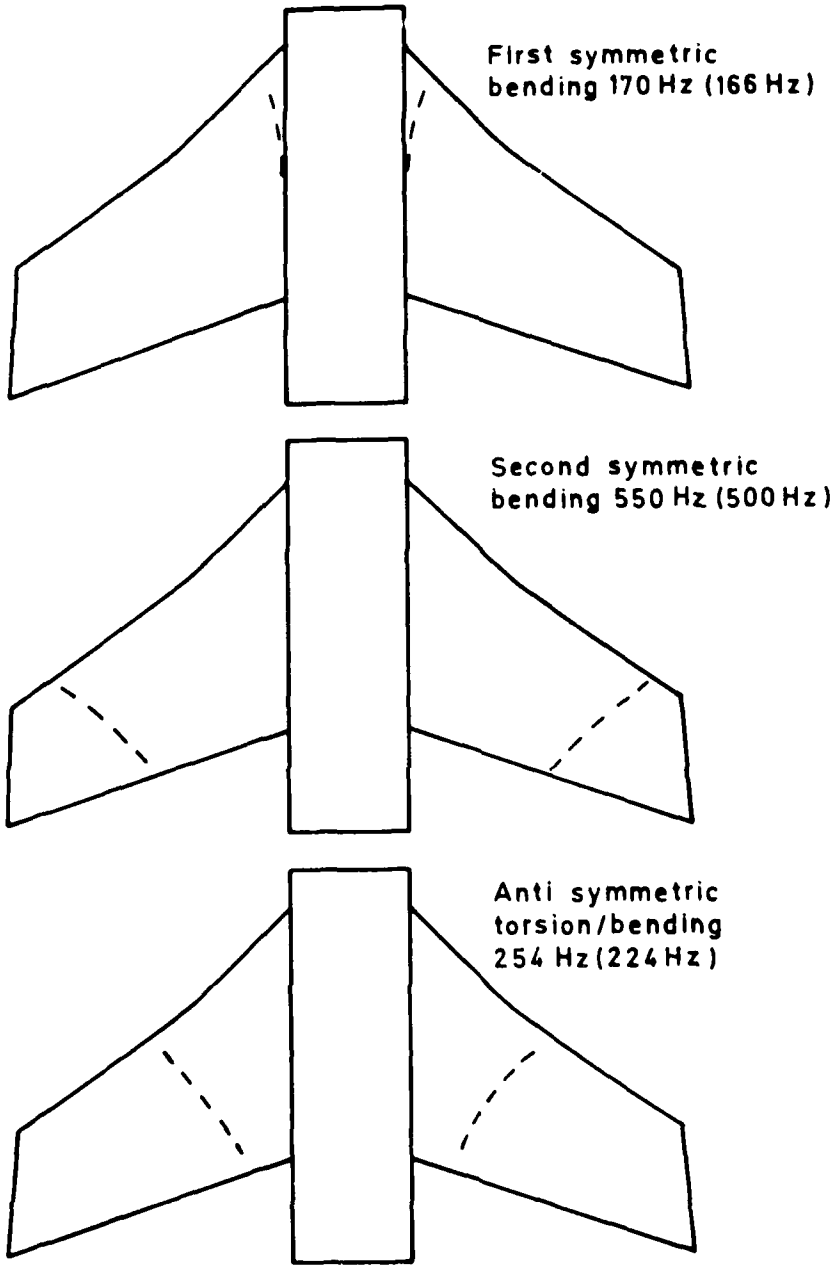

Roll freedom - clamp off

Frequencies in brackets - with stores

Fig 2 Wing modes – wind off

TR 82007

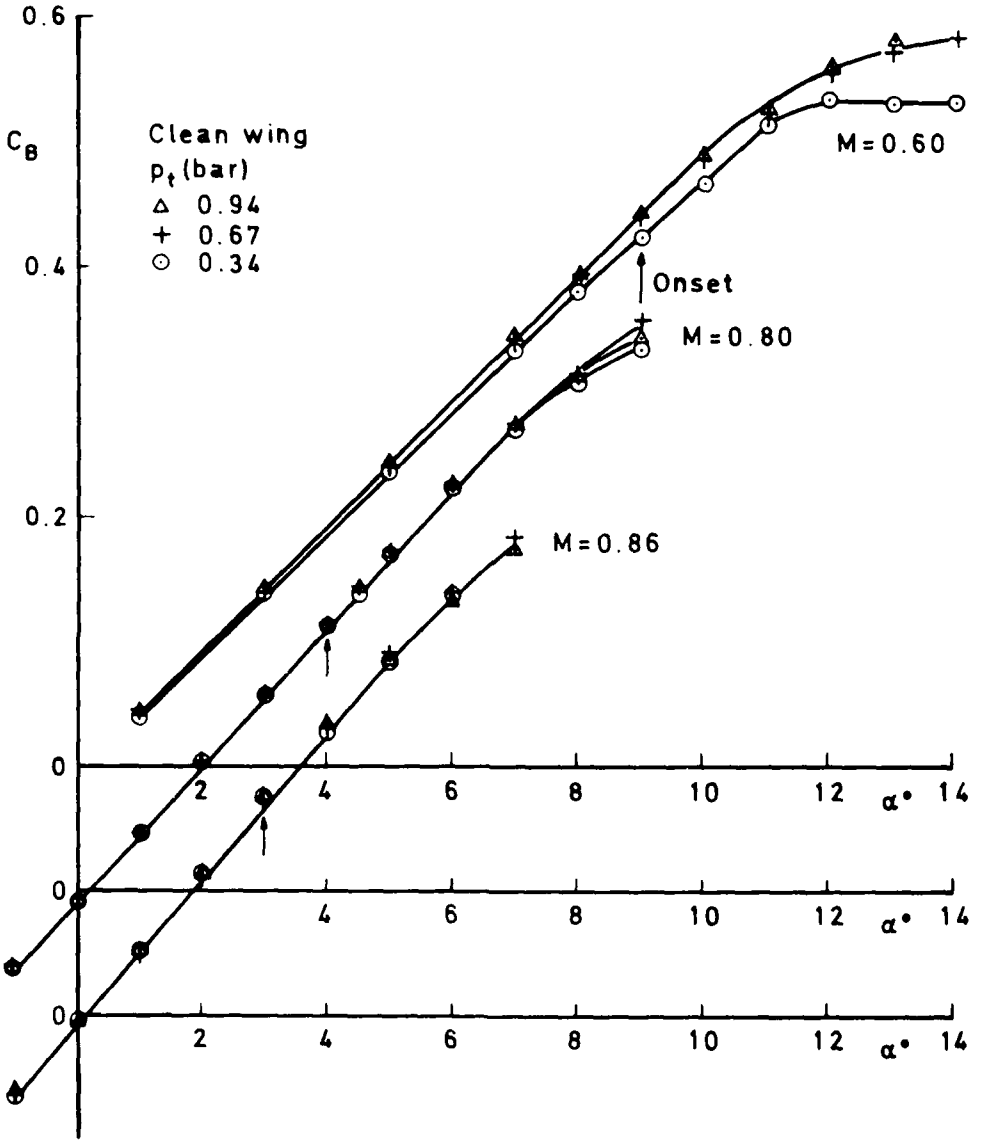

Fig 3 Steady bending moment coefficient v incidence — no roll freedom

Fig 4

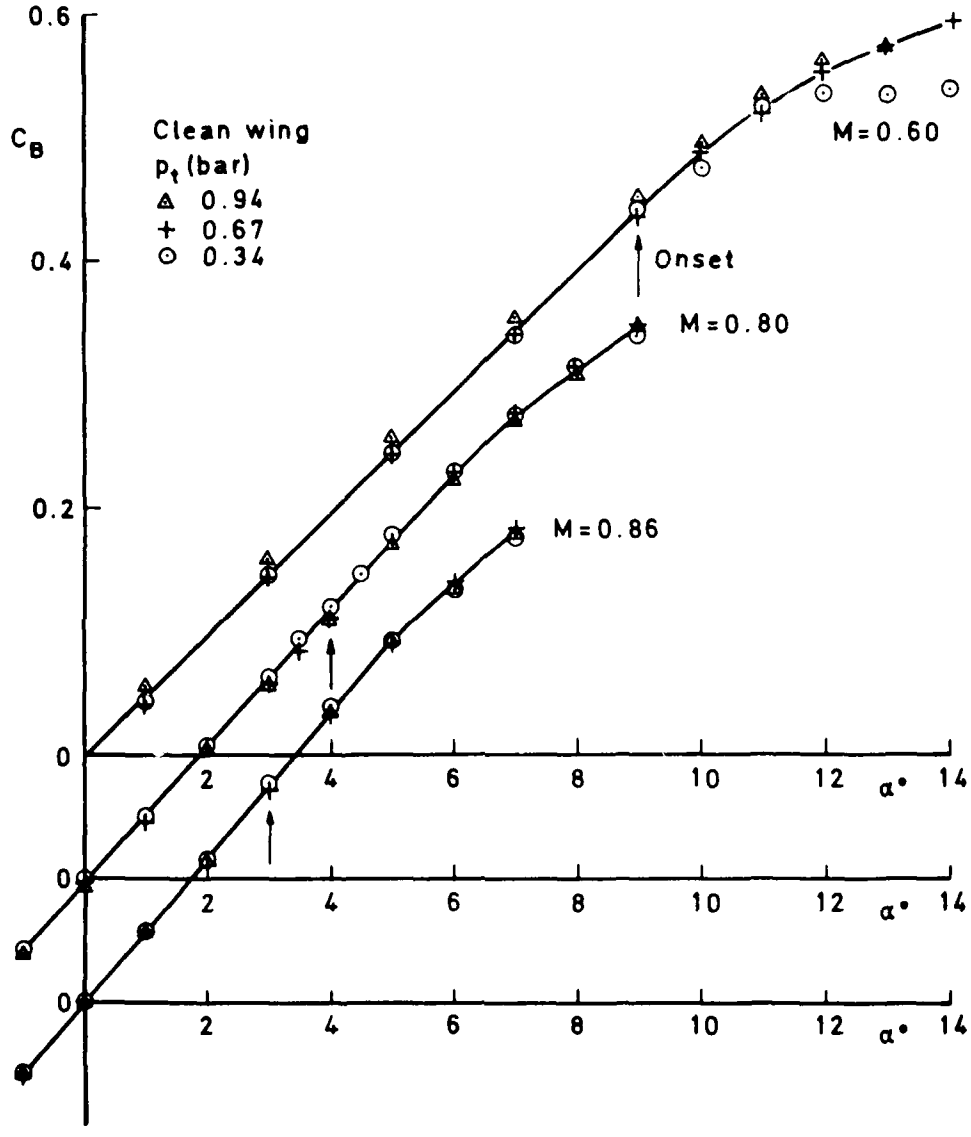

Fig 4 Steady bending moment coefficient v incidence — with roll freedom

TR 82007

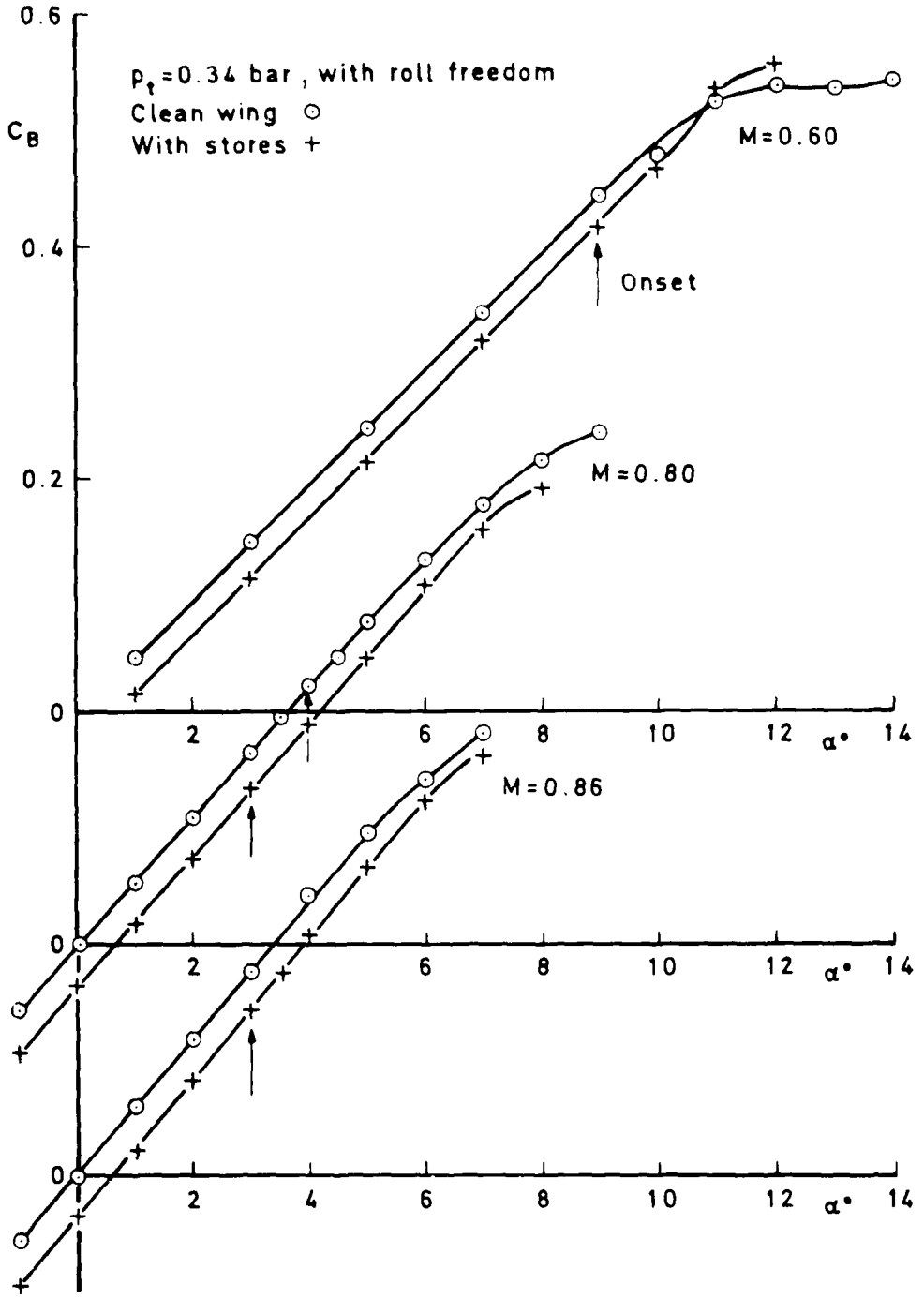

Fig 5 Influence of stores on steady bending moment coefficient

Fig 6

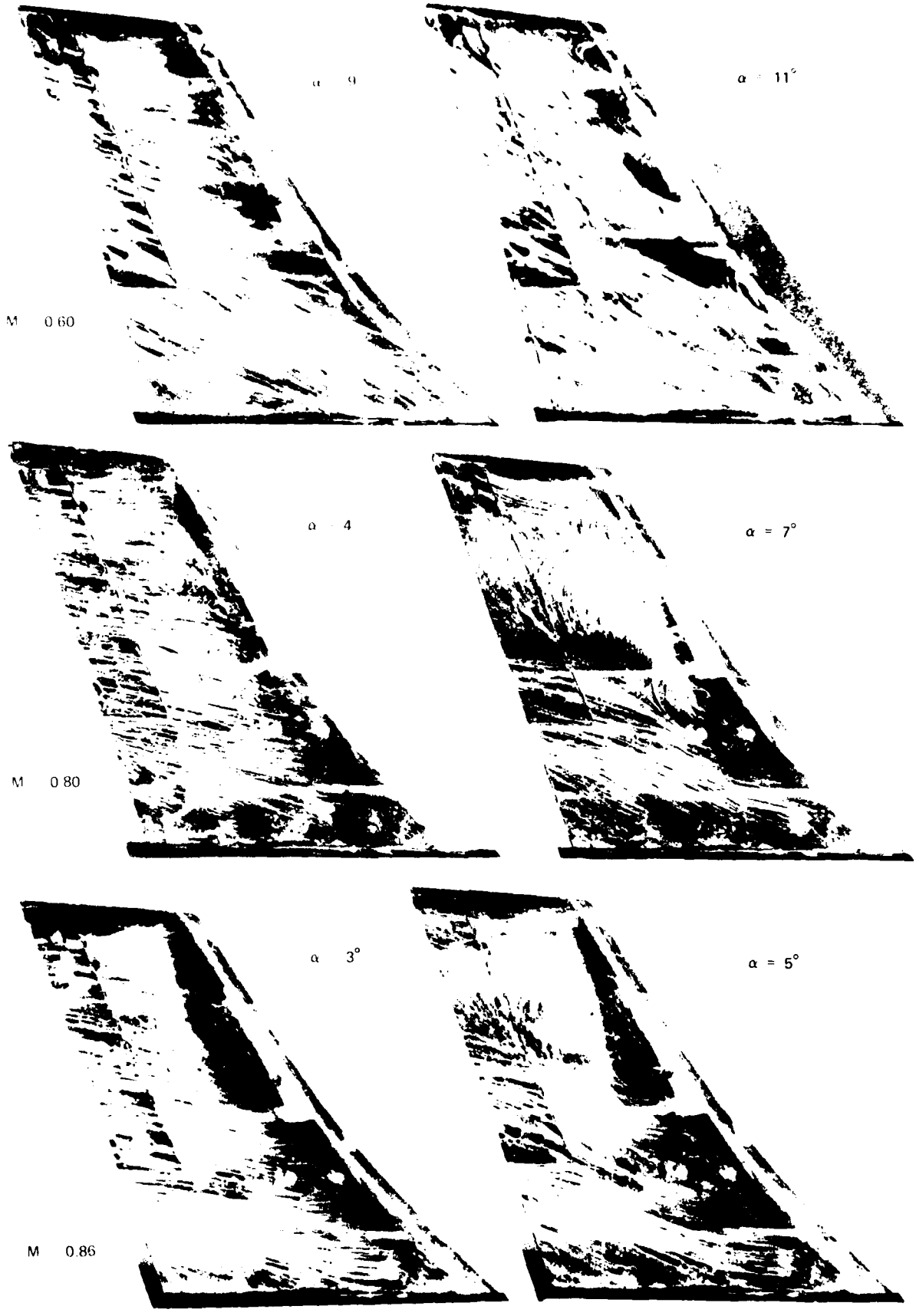

Fig 6 Typical oil flow photographs (p_t = 0.94 bar)

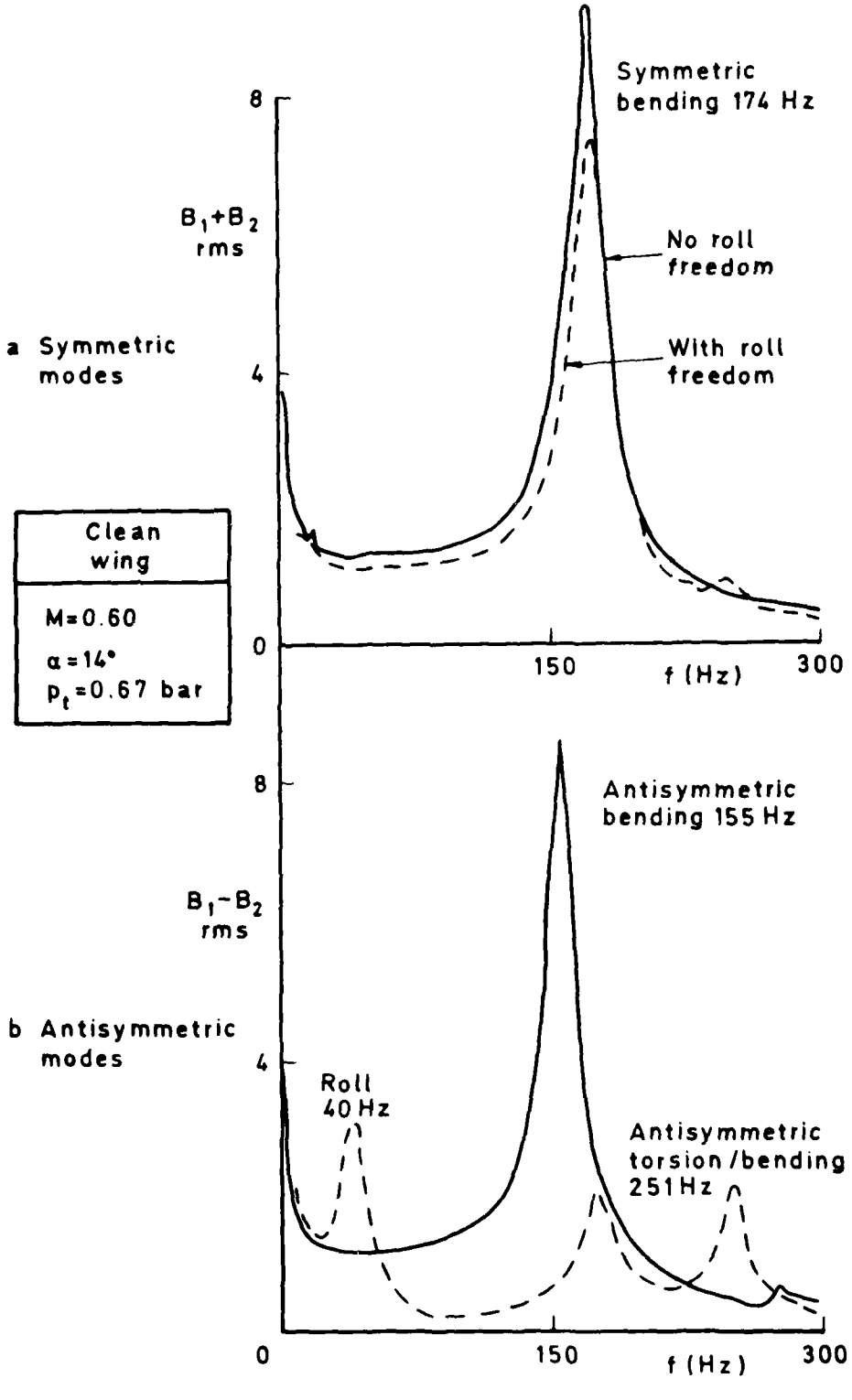

Fig 7a&b Typical spectra of combined wing-root strain signals

TR 82007

Fig 8a-c

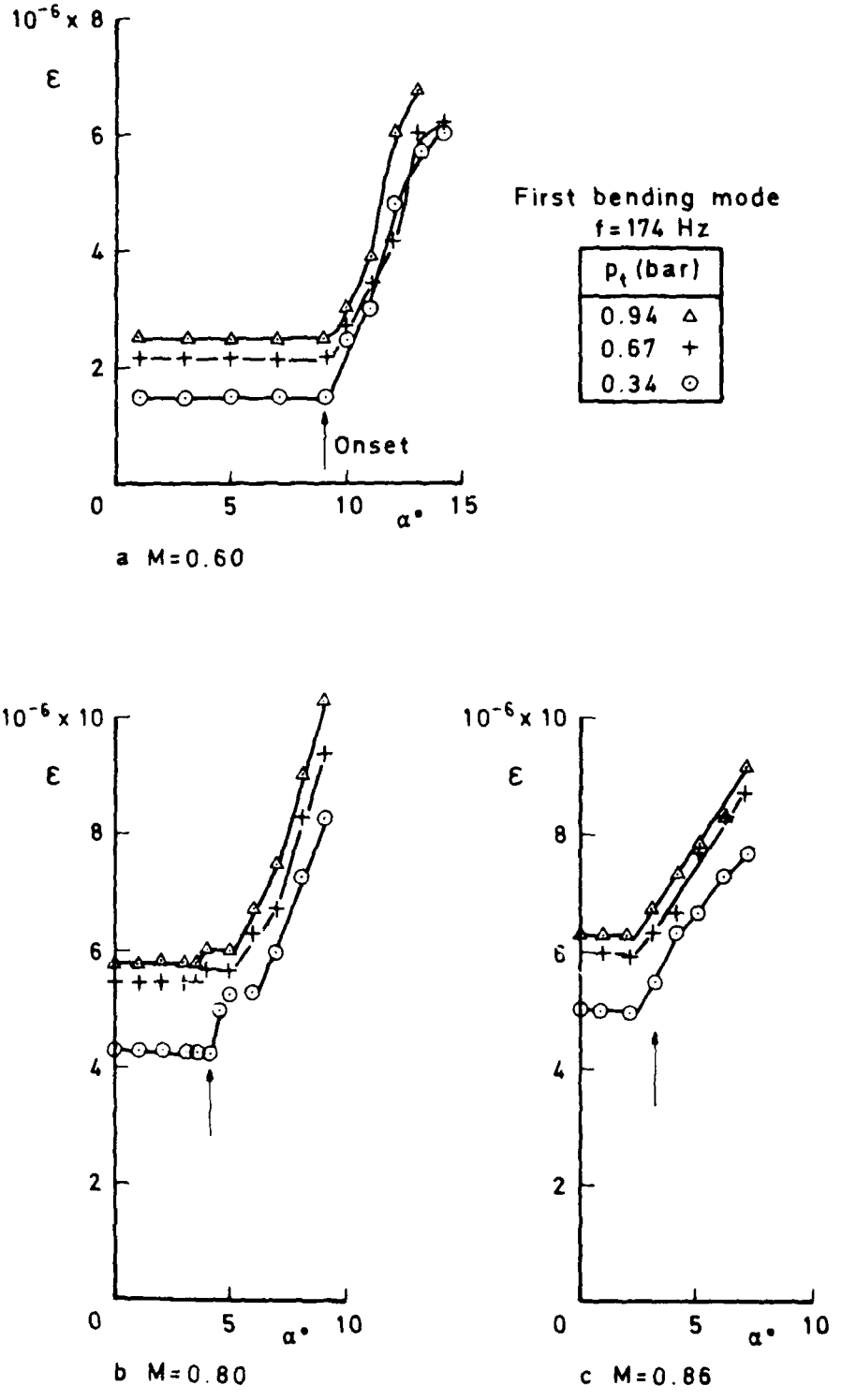

Fig 8a-c Unsteady wing-root strain v incidence

TR 82007

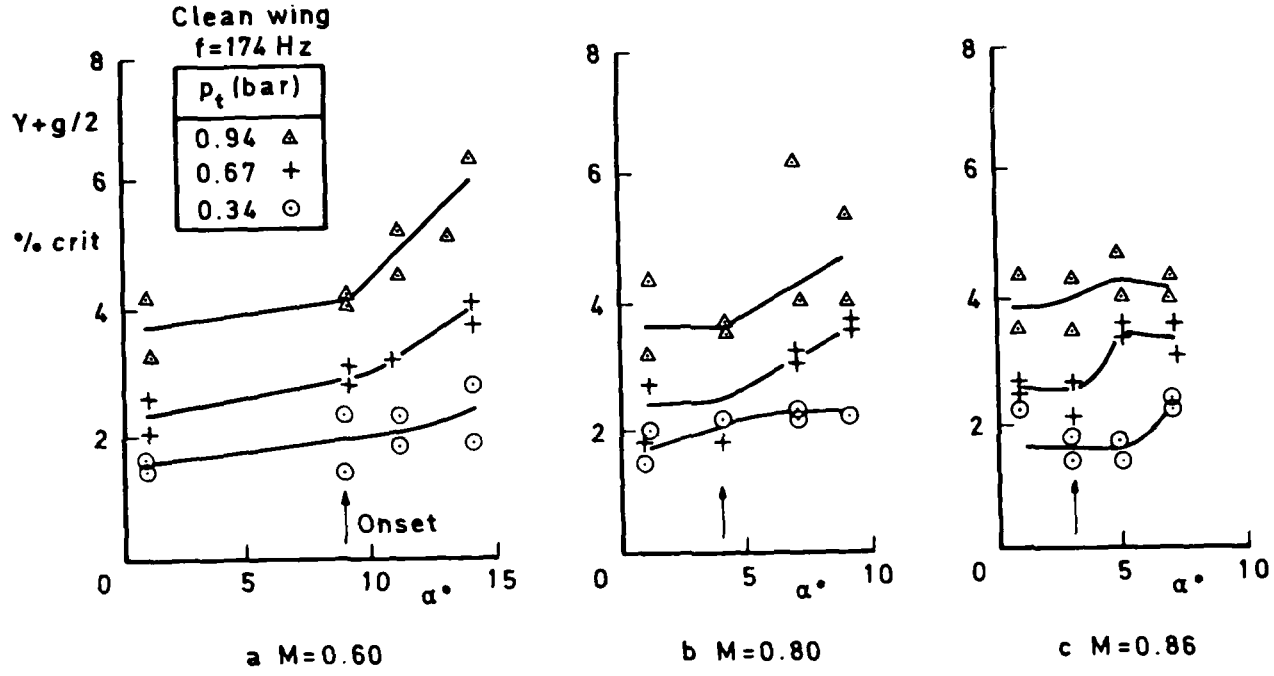

Fig 9a-c First symmetric bending – damping – v incidence

Fig 9a-c

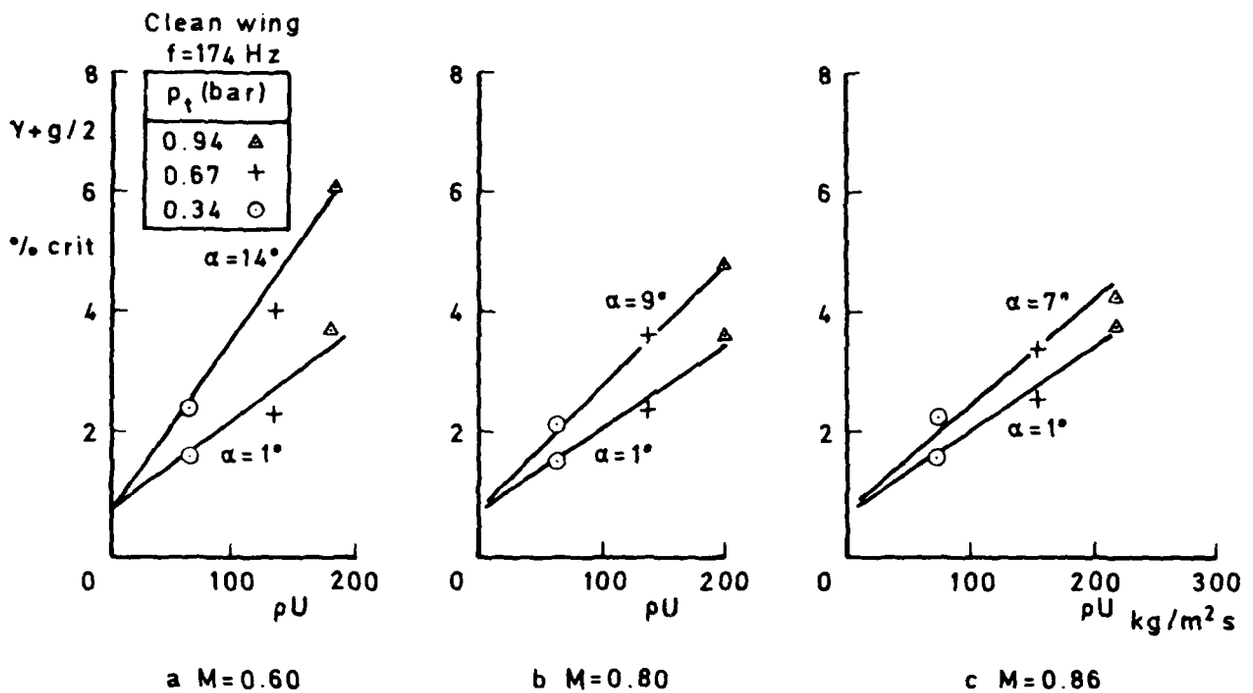

Fig 10a-c First symmetric mode – damping v product of density x velocity

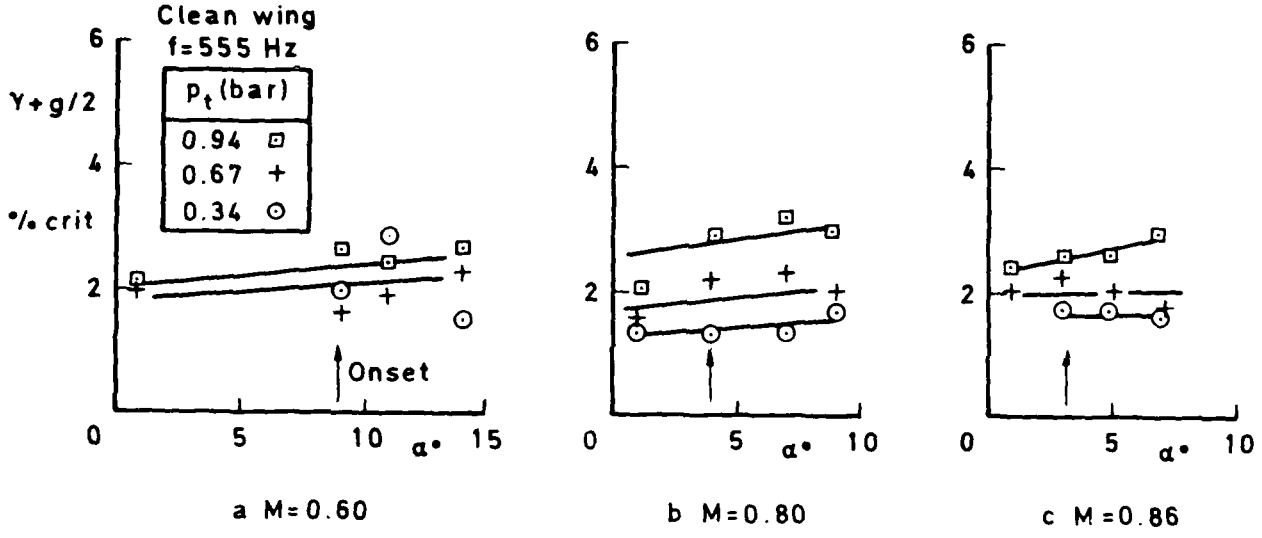

Fig 11a-c Second symmetric bending mode – damping v incidence

Fig 12a-c

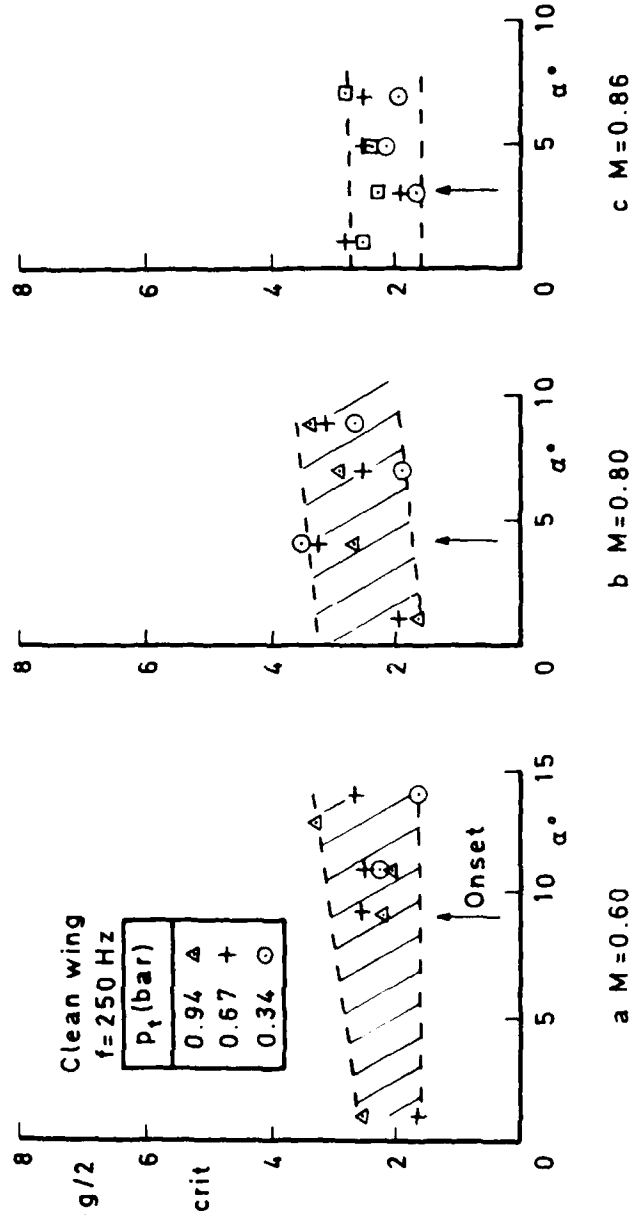

Fig 12a-c First anti-symmetric bending/torsion mode – damping v incidence

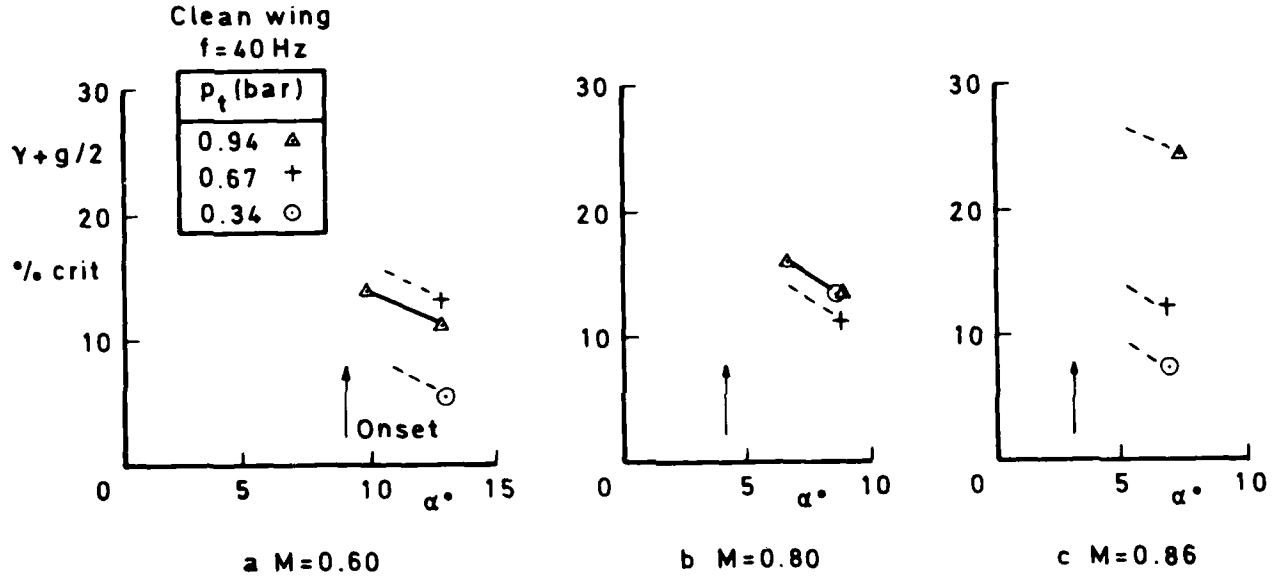

Fig 13a-c Rigid body roll damping v incidence

Fig 14a-c

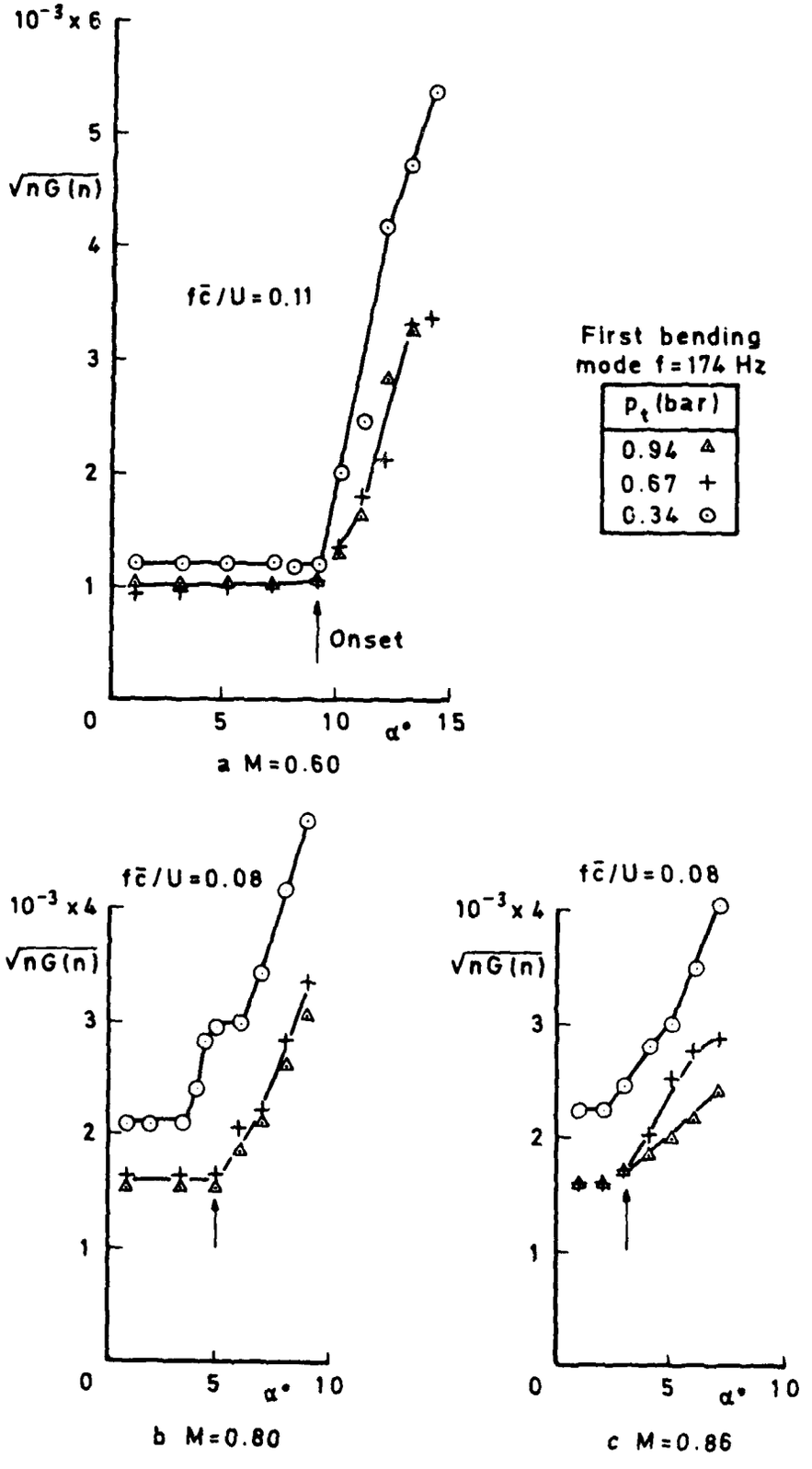

Fig 14a-c Buffet excitation parameter v incidence

TR 82007

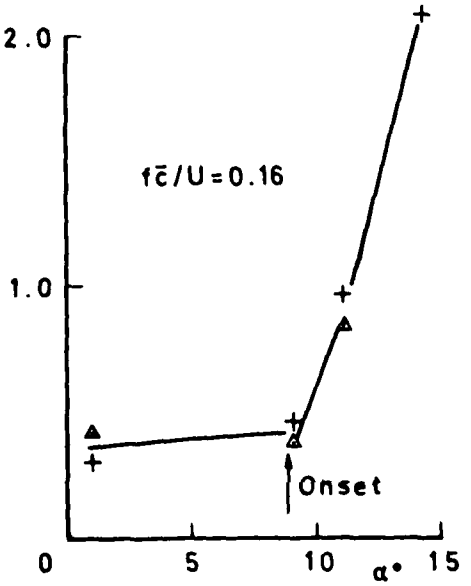

a Antisymmetric combined torsion/bending f=250 Hz

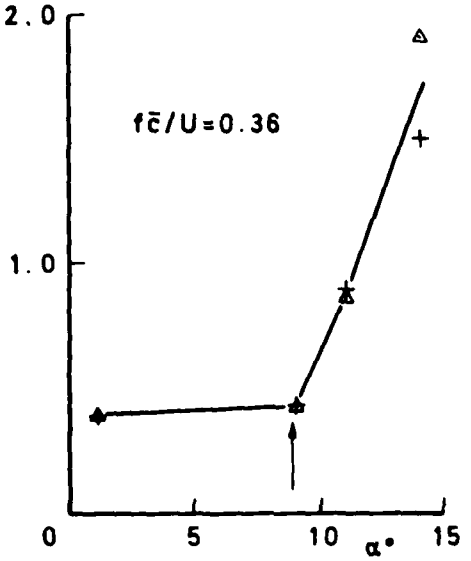

b Symmetric overtone bending f=555 Hz

M=0.60

p_t (bar)	
0.94	△
0.67	+

Fig 15a&b Buffet excitation parameter v incidence — high frequency modes

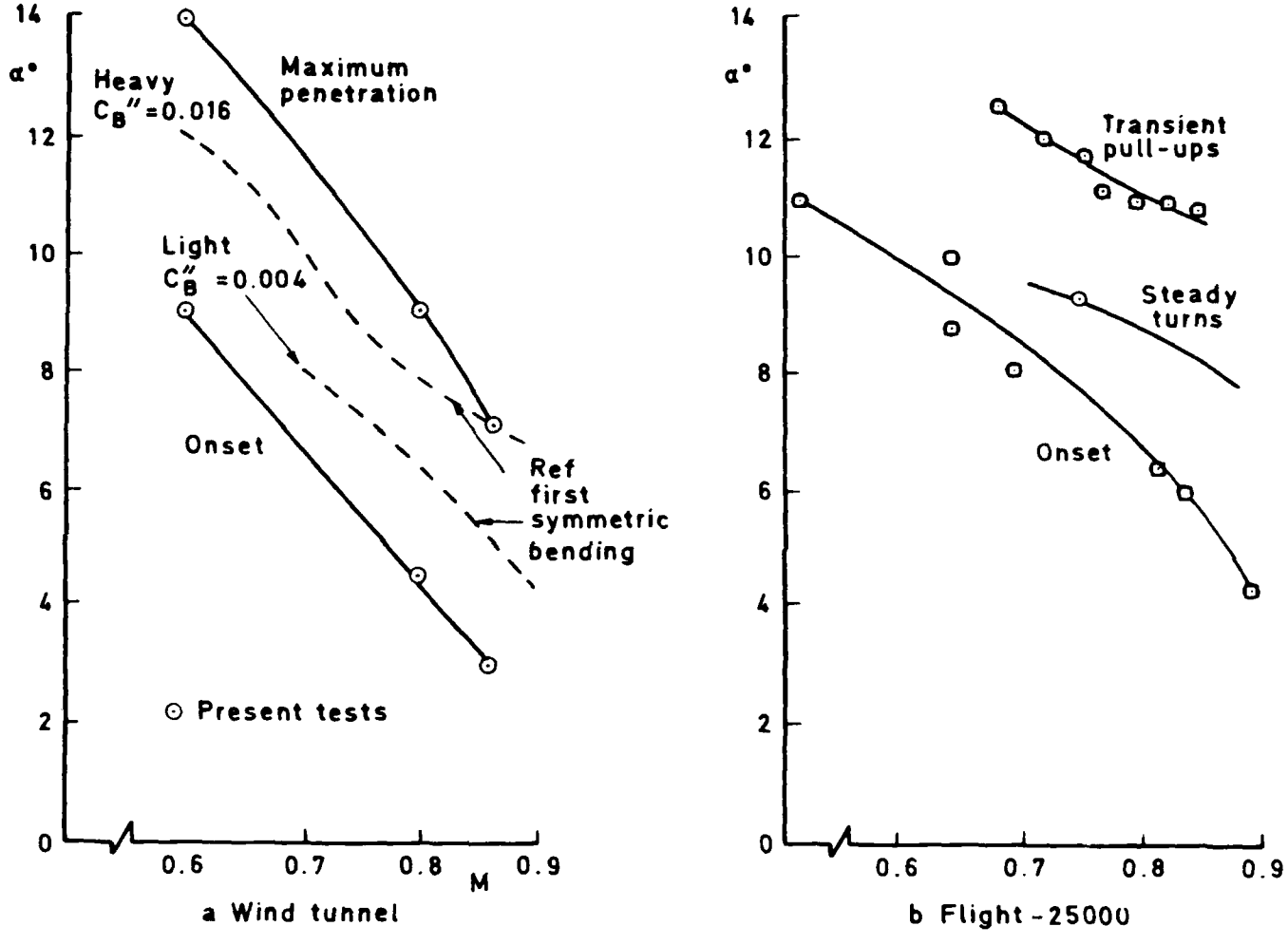

Fig 16a&b Comparison of funnel and flight buffet boundaries

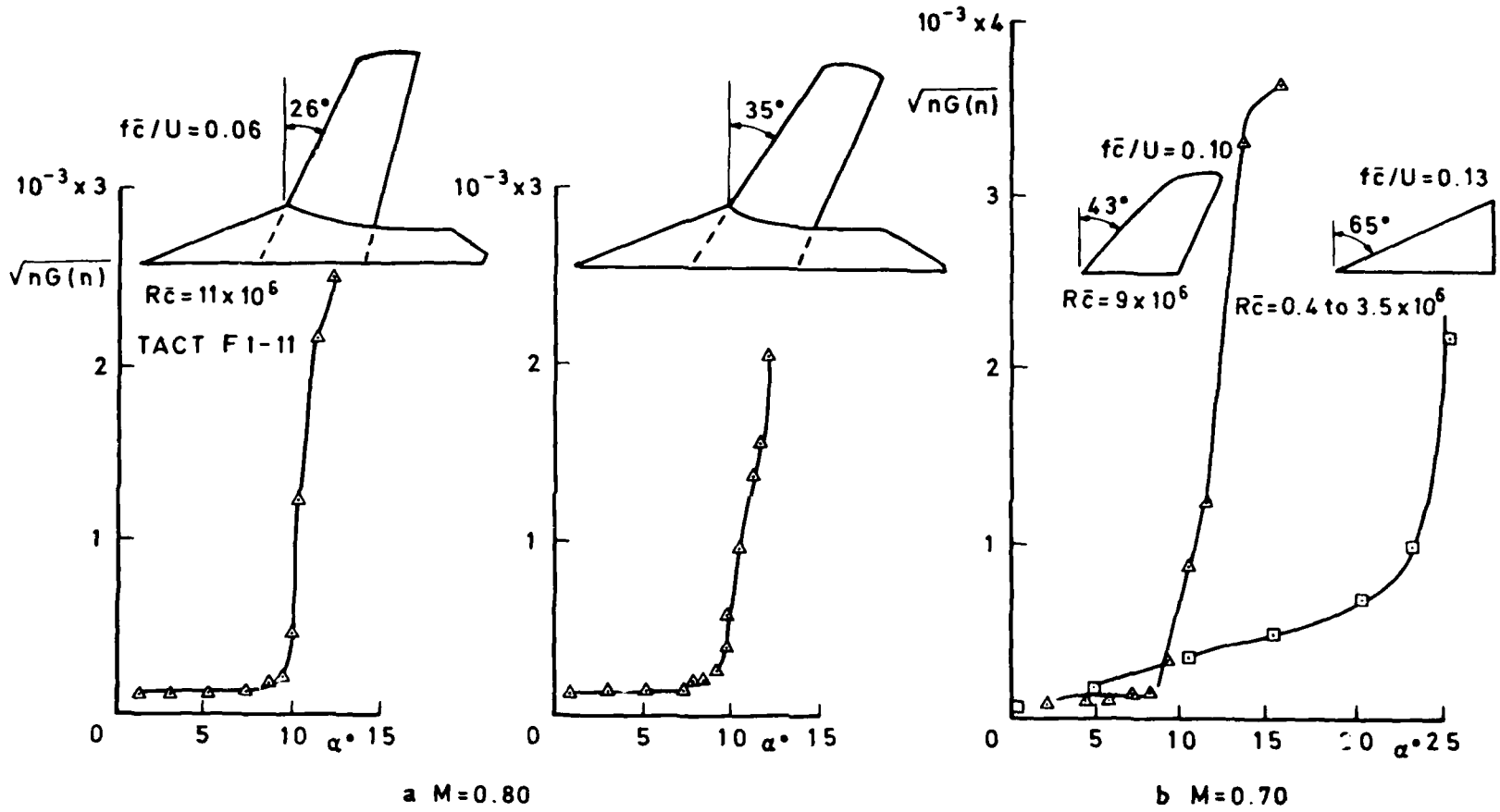

Fig 17a&b Buffet excitation parameters for ordinary wind tunnel models (first bending mode)

Fig 17a&b

Fig 18

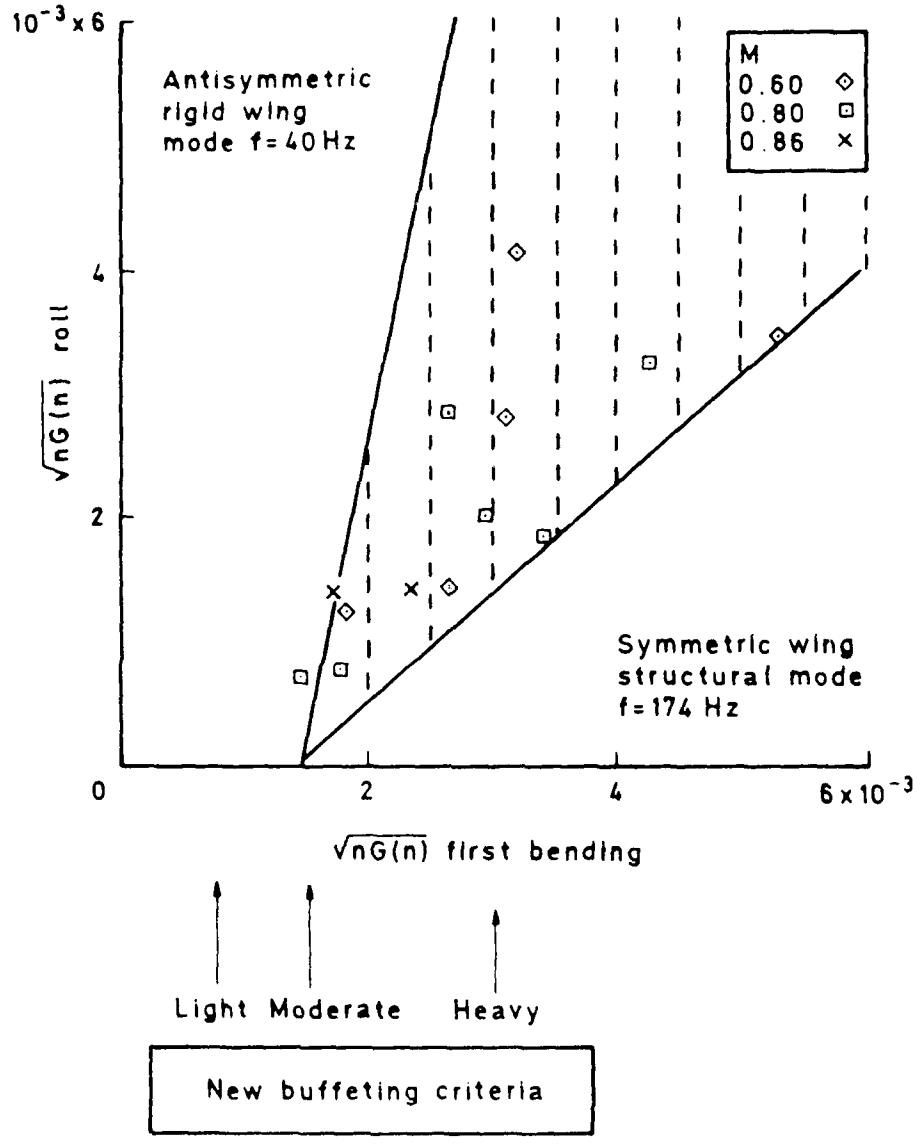

Fig 18 Correlation between buffet excitation parameter in roll and bending modes

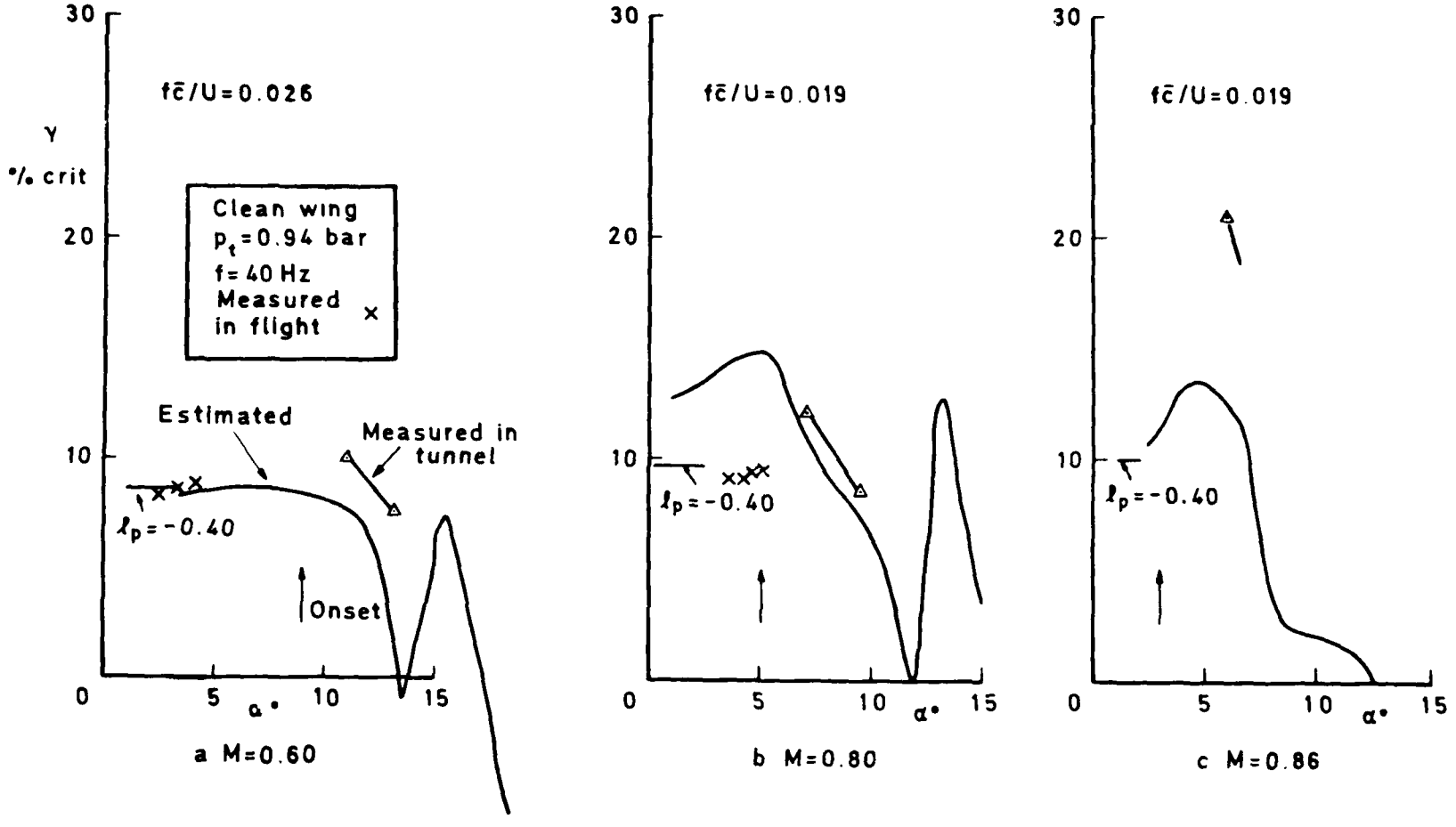

Fig 19a-c Comparison of estimated and measured aerodynamic damping in roll

Fig 19a-c

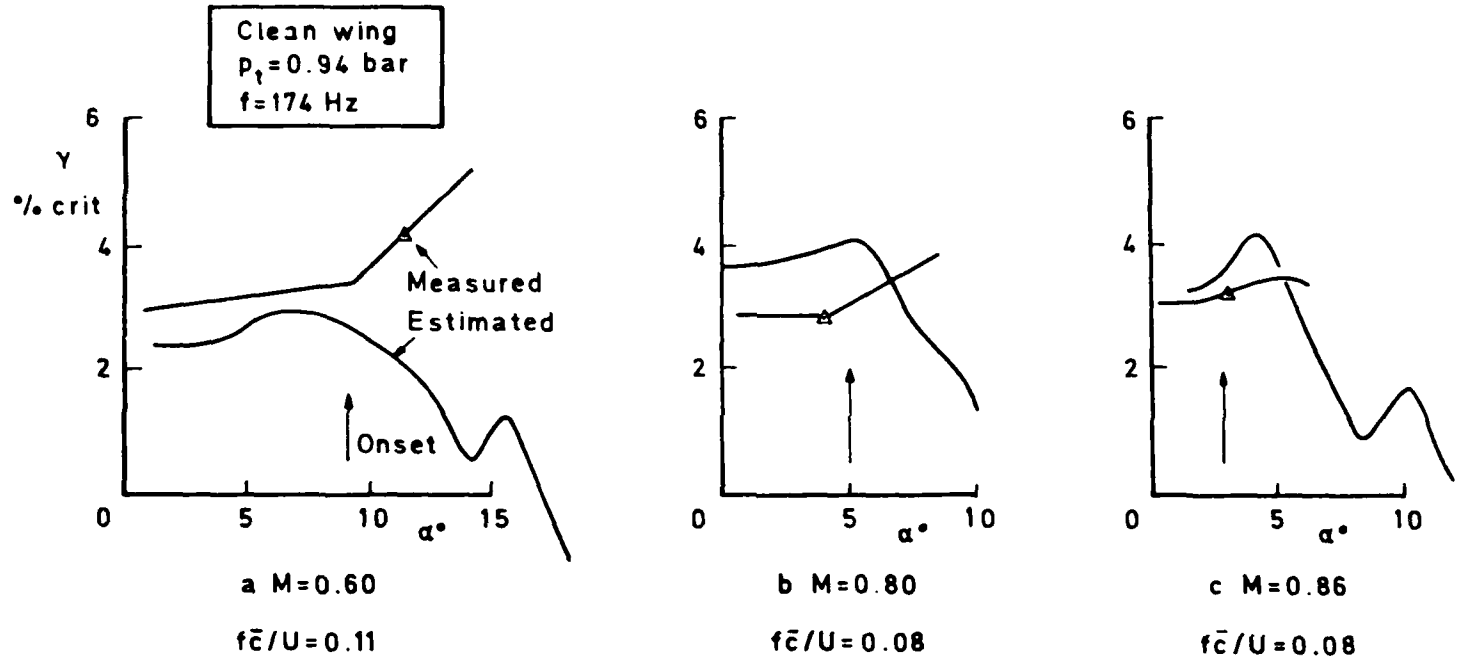

Fig 20a-c Comparison of estimated and measured aerodynamic damping in first symmetric bending

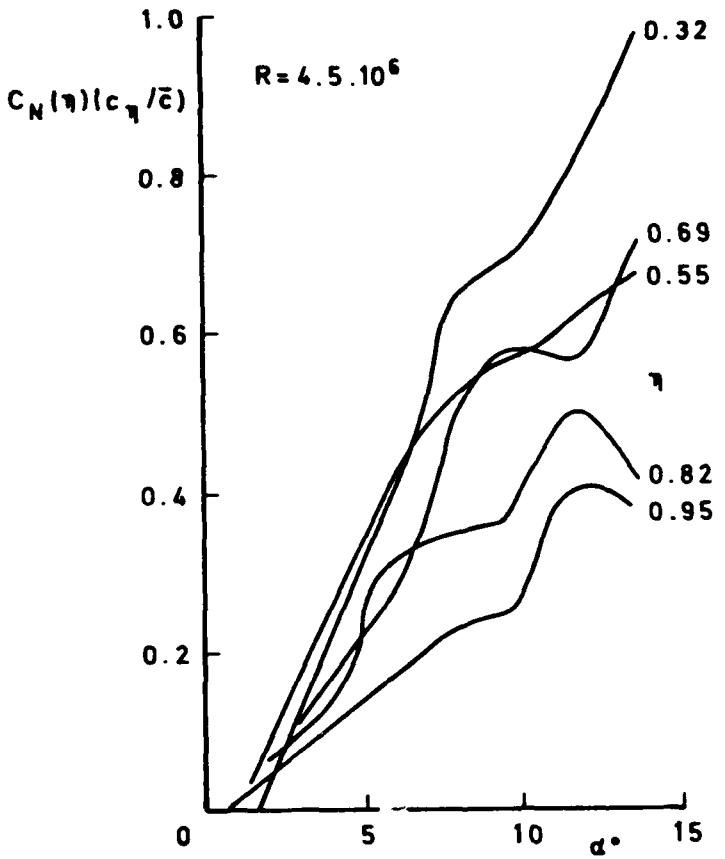

a Normal force coefficient x local chord ratio ratio vs angle of incidence

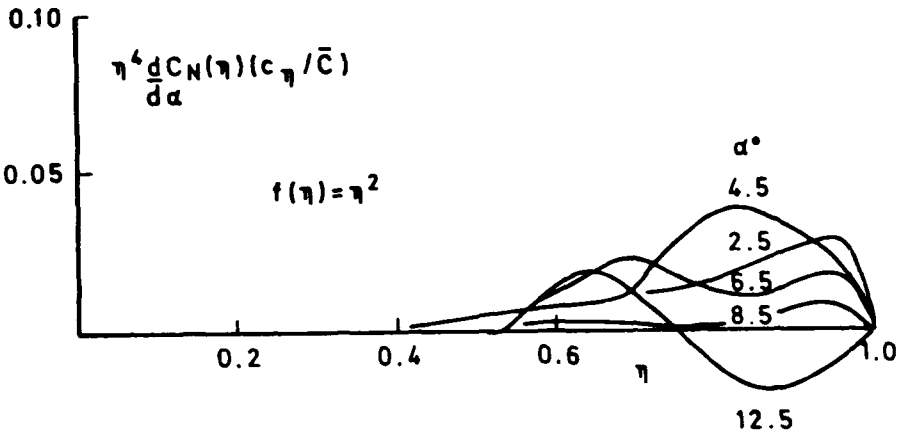

b Ordinate for I vs spanwise position

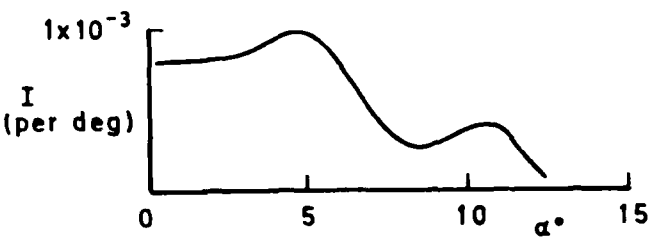

c Variation of integral with angle of incidence

Fig 21a-c Quasi-steady estimate of aerodynamic damping for first symmetric bending, M = 0.85


MED
8